THE JOURNAL OF BIOLOGICAL CHEMISTRY VOL. 288, NO. 40, pp. 28668–28686, October 4, 2013
Published in the U.S.A.

Nox4 NADPH Oxidase Mediates Peroxynitrite-dependent Uncoupling of Endothelial Nitric-oxide Synthase and Fibronectin Expression in Response to Angiotensin II

*ROLE OF MITOCHONDRIAL REACTIVE OXYGEN SPECIES**

Received for publication, March 19, 2013, and in revised form, July 23, 2013 Published, JBC Papers in Press, August 12, 2013, DOI 10.1074/jbc.M113.470971

Doug-Yoon Lee[‡1], Fabien Wauquier[‡1], Assaad A. Eid[‡], Linda J. Roman[§], Goutam Ghosh-Choudhury[‡¶‖2], Khaled Khazim[‡], Karen Block[‡‖], and Yves Gorin[‡3]

From the Departments of [‡]Medicine and [§]Biochemistry, University of Texas Health Science Center, the [¶]Veterans Administration Research and Geriatric Research, Education and Clinical Center, and the [‖]Audie Leon Murphy Memorial Hospital Division, South Texas Veterans Health Care System, San Antonio, Texas 78229

Background: Oxidative stress is critical for the fibrotic response of mesangial cells (MCs) to angiotensin II.
Results: Nox4- and mitochondrial reactive oxygen species (ROS)-dependent endothelial nitric-oxide synthase (eNOS) uncoupling led to fibronectin accumulation in MCs stimulated by angiotensin II.
Conclusion: The Nox4/mitochondrial ROS/eNOS pathway mediates angiotensin II-induced MC injury.
Significance: Targeting Nox4 and mitochondrial ROS is a promising therapeutic approach.

Activation of glomerular mesangial cells (MCs) by angiotensin II (Ang II) leads to extracellular matrix accumulation. Here, we demonstrate that, in MCs, Ang II induces endothelial nitric-oxide synthase (eNOS) uncoupling with enhanced generation of reactive oxygen species (ROS) and decreased production of NO. Ang II promotes a rapid increase in 3-nitrotyrosine formation, and uric acid attenuates Ang II-induced decrease in NO bioavailability, demonstrating that peroxynitrite mediates the effects of Ang II on eNOS dysfunction. Ang II rapidly up-regulates Nox4 protein. Inhibition of Nox4 abolishes the increase in ROS and peroxynitrite generation as well as eNOS uncoupling triggered by Ang II, indicating that Nox4 is upstream of eNOS. This pathway contributes to Ang II-mediated fibronectin accumulation in MCs. Ang II also elicits an increase in mitochondrial abundance of Nox4 protein, and the oxidase contributes to ROS production in mitochondria. Overexpression of mitochondrial manganese superoxide dismutase prevents the stimulatory effects of Ang II on mitochondrial ROS production, loss of NO availability, and MC fibronectin accumulation, whereas manganese superoxide dismutase depletion increases mitochondrial ROS, NO deficiency, and fibronectin synthesis basally and in cells exposed to Ang II. This work provides the first evidence that uncoupled eNOS is responsible for Ang II-induced MC fibronectin accumulation and identifies Nox4 and mitochondrial ROS as mediators of eNOS dysfunction. These data shed light on molecular processes underlying the oxidative signaling cascade engaged by Ang II and identify potential targets for intervention to prevent renal fibrosis.

Extracellular matrix accumulation in glomeruli contributes to the pathogenesis of glomerulosclerosis in fibrotic renal diseases (1–4). Up-regulation of the renin-angiotensin system plays a key role in the initiation and the progression of glomerular injury via induction of extracellular matrix expansion in glomerular mesangial cells (MCs)[4] (4–10). The octapeptide hormone angiotensin II (Ang II) is the dominant renin-angiotensin system effector and is implicated in the pathogenesis of fibrosis of the glomerular microvascular bed (4–10).

Oxidative stress has emerged as a critical pathogenic factor in the development of renal and vascular diseases (4–14). The Nox family of NADPH oxidases and mitochondria are the major sources of reactive oxygen species (ROS) in the vasculature and the kidney that contribute to the development of pathological conditions (10–19). The Nox proteins correspond to homologues of gp91^{phox} (or Nox2), the catalytic moiety found in phagocytes (11–13, 15). Seven members of the Nox family have been identified in the human genome: Nox1 to Nox5 and the dual oxidases Duox1 and Duox2 (11–15). The homologue Nox4 (NADPH oxidase 4) plays a key role in vascular and renal cell injury, including the fibrotic processes (10–14, 20–26). However, the mechanisms that Nox4 utilize to exert this bio-

* This work was supported, in whole or in part, by National Institutes of Health Grants RO1 DK 079996 (to Y. G.), RO1 CA 131272 (to K. B.), and RO1 DK 50190 (to G. G. C.). This work was also supported in part by a Juvenile Diabetes Research Foundation Multiproject Grant (to Y. G. and K. B.), a Juvenile Diabetes Research Foundation Advanced Research Fellowship Grant (to A. A. E.), and Veterans Administration Merit Awards (to K. B. and G. G. C.).

[1] These authors contributed equally to this work.

[2] Recipient of Veterans Administration Senior Research Career Scientist Award.

[3] To whom correspondence should be addressed: Dept. of Medicine, Division of Nephrology MC 7882, University of Texas Health Science Center, 7703 Floyd Curl Dr., San Antonio, TX 78229-3900. Tel.: 210-567-4700; Fax: 210-567-4712; E-mail: gorin@uthscsa.edu.

[4] The abbreviations used are: MC, mesangial cell; AdβGal, adenovirus encoding β-Galactosidase; Ang II, angiotensin II; cGMP, cyclic GMP; DHE, dihydroethidium; eNOS, endothelial nitric-oxide synthase; EOH, 2-hydroxy-ethidium; iNOS, inducible nitric-oxide synthase; L-NAME, N^G-nitro-L-arginine methyl ester; Mit, mitochondria; MnSOD, mitochondrial manganese-dependent superoxide dismutase; AdMnSOD, adenovirus encoding MnSOD; nNOS, neuronal nitric-oxide synthase; ROS, reactive oxygen species; Scr, nontargeting siRNA; BH_4, (6*R*)-5,6,7,8-tetrahydrobiopterin; sieNOS, siRNA oligonucleotides for eNOS; siNox4, siRNA for Nox4; DTPA, diethylenetriaminepentaacetic acid.

logical effect remain unclear, and the downstream effectors of the oxidase are not well defined.

Endothelial nitric-oxide synthase (eNOS), which generates NO in the presence of optimal concentrations of the substrate L-arginine and the cofactor (6*R*)-5,6,7,8-tetrahydrobiopterin (BH_4), constitutes a major defense against vascular injury (27–30). Under pathological conditions, diminished levels of BH_4 or L-arginine promote the transfer of electrons to molecular oxygen instead of L-arginine to produce superoxide rather than NO, a phenomenon referred to as "uncoupling" (27–30). Although uncoupling of eNOS and decrease in NO bioavailability has been implicated in cardiovascular diseases (27–30), the role of eNOS dysfunction in renal pathology remains unclear. The protective role of NO generation by eNOS in the kidney was demonstrated by recent studies showing that eNOS knock-out mice made diabetic develop advanced lesions (31–33). eNOS is expressed in MCs, and its uncoupling has been linked to the decline in NO levels observed in the diabetic environment (34–36). A role of Ang II in eNOS uncoupling and the decrease in renal NO production is suggested by the observations that angiotensin II type 1 receptor blockade restores eNOS function and NO levels in experimental models of diabetes (37, 38). However, the molecular mechanisms by which eNOS function and NO bioavailability are altered by Ang II in renal cells are unknown. The present study defines novel molecular mechanisms whereby Ang II promotes fibrotic events in renal cells and provides a rationale for the prevention of Nox4- and mitochondrial ROS-dependent eNOS dysfunction as a therapeutic intervention for the treatment of renal fibrotic diseases.

EXPERIMENTAL PROCEDURES

Cell Culture, Transfections, and Adenovirus Infection

Rat glomerular MCs were isolated and characterized as described (20, 21, 24–26). These cells were used between 15th and 30th passages. Selected experiments were performed in primary and early passaged MCs to confirm the data obtained with late passages. The cells were maintained in DMEM supplemented with antibiotic/antifungal solution and 17% fetal bovine serum.

For the RNA interference experiments, a SMARTpool consisting of four short or siRNA duplexes specific for rat Nox4 or eNOS was obtained from Dharmacon. The SMARTpool of siRNAs was introduced into the cells by double transfection using X-tremeGENE (Roche Applied Science) as described (21, 26). The siRNAs for Nox4 or eNOS were used at a concentration of 100 nM. Scrambled siRNAs (nontargeting siRNA) (100 nM) served as controls to validate the specificity of the siRNAs. Adenovirus encoding for wild type mitochondrial manganese-dependent superoxide dismutase (AdMnSOD) was used to infect MCs as previously described (26, 39, 40). As a control for the effects of adenovirus infection alone, an adenovirus encoding β-Galactosidase (Adβ Gal) was used.

Western Blotting Analysis

MCs grown to near confluence were made quiescent by serum deprivation for 48 h and treated or not with 1 μM Ang II for the specified duration in serum-free Dulbecco's modified Eagle's medium at 37 °C. The cells were lysed in radioimmune precipitation buffer at 4 °C for 30 min. The cell lysates were centrifuged at 10,000 × *g* for 30 min at 4 °C. Protein was determined in the cleared supernatant using the Bio-Rad protein assay reagent.

For immunoblotting, proteins were separated using SDS-PAGE and transferred to polyvinylidene difluoride membranes. The membranes were blocked with 5% low fat milk in Tris-buffered saline and then incubated with a rabbit polyclonal eNOS antibody (catalogue nos. ADI-KAP-NO020 and KAP-NO002; Enzo Life Sciences/Stressgen) (dilution 1:1,000), a rabbit monoclonal nNOS antibody (catalogue no. 2081-1; Abcam/Epitomics Inc.), a rabbit polyclonal iNOS antibody (catalogue no. 61033; BD Biosciences), a rabbit polyclonal anti-3-nitrotyrosine (catalogue no. 06-284; EMD Millipore) (1:1,000), a rabbit polyclonal Nox4 antibody directed against recombinant glutathione *S*-transferase mouse Nox4-(299–515) designed in our laboratory (dilution 1:1,000) (20, 21, 26), a rabbit polyclonal Nox4 antibody (catalogue no. H-300; Santa Cruz Biotechnology, Inc.) (1:300), a rabbit polyclonal MnSOD (SOD2) antibody (catalogue no. ab86087; Abcam/Epitomics Inc.) (1:1,000), a rabbit polyclonal anti-fibronectin antibody (catalogue no. F3648; Sigma) (1:2,500), a rabbit polyclonal anti-GAPDH (catalogue no. G9545; Sigma) (1:1,000), or a mouse monoclonal anti-β-actin (1:4,000) (catalogue no. A2066; Sigma). The appropriate horseradish peroxidase-conjugated secondary antibodies were added, and bands were visualized by enhanced chemiluminescence. Densitometric analysis was performed using National Institutes of Health Image software (21, 26).

Mitochondria Isolation Kit

MCs were harvested from the cultures and fractionated into cytosol and mitochondria (Mit) by using a Pierce mitochondria isolation kit (Pierce) according to the instructions of the manufacturer as previously described (21).

Assay of eNOS Dimer/Monomer

SDS-resistant eNOS dimers and monomers were assayed by using low temperature SDS-PAGE as described previously (41). Briefly, after being washed twice with ice-cold phosphate-buffered saline, Ang II-treated MCs were lysed as described above, and protein lysates were mixed with loading buffer and loaded on gels without boiling. Proteins were separated with low temperature SDS-PAGE under reducing conditions (with β-mercaptoethanol). Gels and buffers were kept at 4 °C during the whole procedure.

Immunofluorescence Confocal Microscopy

MCs grown on 4-well chamber slides were fixed with 4% paraformaldehyde for 15 min and permeabilized with 0.2% Triton X-100 for 5 min. The cells were then blocked with 5% normal goat serum or 5% normal donkey serum in phosphate-buffered saline for 30 min and incubated with appropriate primary antibodies (anti-eNOS, anti-3-nitrotyrosine, anti-fibronectin, or anti-MnSOD) for 30 min. Cyanin-3- or fluorescein isothiocyanate-conjugated secondary antibodies were then applied to the appropriate cells for 30 min. The cells were washed three times with phosphate-buffered saline, mounted with antifade

reagent with 4′,6-diamidino-2-phenylindole, and visualized on an Olympus FV-500 confocal laser scanning microscope. To estimate the brightness intensity of 3-nitrotyrosine and fibronectin signals, groups of cells randomly selected from the digital image were outlined (at least five groups for each sample), and the average brightness of the enclosed area was semiquantified using either the Image-Pro Plus 4.5 software (Media Cybernetics) or National Institutes of Health Image/ImageJ software, as described (20, 21, 26). The data shown represent three separate experiments and are expressed as relative fluorescence intensity.

NADPH Oxidase Assay

NADPH oxidase activity was measured by the lucigenin-enhanced chemiluminescence method as described (20, 21, 24). Briefly, MCs grown in serum-free medium for 48 h and treated or not with 1 μM Ang II for the indicated time periods were washed five times in ice-cold phosphate-buffered saline and were scraped from the plate in the same solution followed by centrifugation at 800 $\times$ *g*, 4 °C, for 10 min. The cell pellets were resuspended in lysis buffer. Cell suspensions were homogenized with 100 strokes in a Dounce homogenizer on ice. Homogenates were subjected to a low speed centrifugation at 800 $\times$ *g* at 4 °C for 10 min to remove the unbroken cells and debris, and the aliquots were used immediately. To start the assay, 100 μl of homogenates were added to 900 μl of 50 mM phosphate buffer, pH 7.0, containing 1 mM EGTA, 150 mM sucrose, 5 μM lucigenin, and 100 μM NADPH. Photon emission in terms of relative light units was measured every 20 or 30 s for 10 min in a luminometer. There was no measurable activity in the absence of NADPH. A buffer blank (less than 5% of the cell signal) was subtracted from each reading. Superoxide production was expressed as relative chemiluminescence (light) units/mg of protein. Protein content was measured using the Bio-Rad protein assay reagent.

Detection of ROS Production

Detection of Intracellular Superoxide in MCs Using HPLC—Cellular superoxide production in MCs was assessed by HPLC analysis of dihydroethidium (DHE)-derived oxidation products, as described previously (42). The HPLC-based assay allowed the separation of the superoxide-specific 2-hydroxyethidium (EOH) from the nonspecific ethidium. Briefly, after exposure or not of quiescent MCs grown in 60-mm dishes to 1 μM Ang II for the indicated duration, the cells were washed twice with Hanks' balanced salt solution/DTPA and incubated for 30 min with 50 μM DHE (Sigma-Aldrich) in Hanks' balanced salt solution/100 μM DTPA. Note that for prolonged treatment, the cells were first stimulated with D-glucose and then incubated with DHE. The cells were harvested in acetonitrile and centrifuged (12,000 $\times$ *g* for 10 min at 4 °C). The homogenate was dried under vacuum and analyzed by HPLC with fluorescence detectors (Jasco HPLC system, LC-2000 plus series). Quantification of DHE, EOH, and ethidium concentrations was performed by comparison of integrated peak areas between the obtained and standard curves of each product under identical chromatographic conditions as described. EOH and ethidium were monitored by fluorescence detection with excitation at 510 nm and emission at 595 nm, whereas DHE was monitored by ultraviolet absorption at 370 nm. The results were expressed as produced EOH (nmol) normalized for consumed DHE (*i.e.*, initial minus remaining DHE in the sample) (μmol).

Detection of Intracellular ROS in MCs—ROS generation was also assessed in live cells with DHE (Invitrogen/Molecular Probes) as previously described (25). The cells were loaded with 10 μM DHE in phenol-free DMEM for 30 min at 37 °C. The cells were washed with warm buffer. DHE fluorescent intensity was determined at 520-nm excitation and 610-nm emission and visualized on Olympus FV-500 confocal laser scanning microscope. The brightness intensity of DHE signal was semiquantified by using either the Image-Pro Plus 4.5 software (Media Cybernetics) or National Institutes of Health Image/ImageJ software as described (20, 21, 26). The data shown represent three separate experiments and are expressed as relative fluorescence intensity.

Alternatively, DHE-derived fluorescence was followed in a multiwell fluorescence plate reader. MCs were grown in 12- or 24-well plates and serum-deprived for 48 h. Immediately before the experiments, the cells were washed with phenol red-free DMEM and loaded with 10 μM DHE (Invitrogen/Molecular Probes) dissolved in phenol-free DMEM solution for 15 min at 37 °C. They were then incubated with or without 1 μM Ang II for various time periods. Subsequently, DHE fluorescence was detected at excitation and emission wavelengths of 560 and 635 nm, respectively, and measured with a multiwell fluorescence plate reader (Chameleon Multilabel Detection Platform; Bioscan).

Detection of Mitochondrial ROS in MCs—Mitochondrial superoxide generation was assessed in live cells with MitoSOX Red (Invitrogen/Molecular Probes) (21), which is a fluorogenic dye that is taken up by mitochondria, where it is readily oxidized by superoxide, but not by other reactive oxygen species or reactive nitrogen species. The cells were loaded with 1 μM MitoSOX Red in phenol-free DMEM for 10 min at 37 °C. The cells were washed with warm buffer. MitoSOX Red fluorescent intensity was determined at 515-nm excitation and 580-nm emission. The brightness intensity of MitoSOX signal was semiquantified by using either the Image-Pro Plus 4.5 software (Media Cybernetics) or National Institutes of Health Image/ImageJ software as described (20, 21, 26). The data shown represent three separate experiments and are expressed as relative fluorescence intensity.

Assay of Nitric-oxide Synthase Activity

The nitric oxide-synthesizing activity of NOS was measured with the NOS Detect assay kit (Stratagene) as described previously (43, 44). Briefly, the conversion of L-[^{14}C]arginine (PerkinElmer Life Sciences) to L-[^{14}C]citrulline was used to determine NOS activity in MC lysates, with the addition of the appropriate cofactors, according to the manufacturer's recommendations. Nonspecific production of L-citrulline was monitored by performing the reaction in the presence of N^G-nitro-L-arginine methyl ester (L-NAME), a NOS inhibitor. In the presence of L-NAME, no significant production of NO was observed. Activity is expressed as pmol of citrulline/min/mg of protein.

Quantification of NO Release

MCs were cultured in phenol-free medium. After being serum-starved for 24 h, the cells were treated with 1 μM Ang II for the indicated time. The amount of nitrite, the stable end product of nitric oxide oxidation, was used as an indicator of NO synthesis, catalyzed by eNOS. Nitrite concentration in the culture medium was measured using the Griess reaction with sodium nitrite as a standard, as described (45). The data were expressed corrected for protein content.

Detection of 3-Nitrotyrosine

3-Nitrotyrosine cellular levels were determined in serum-starved MCs treated with or without 1 μM Ang II for the indicated duration by using an enzyme immunoassay kit from OxisResearch™ Products/Percipio Biosciences, Inc. (BIOOXYTECH® Nitrotyrosine-EIA Assay; catalogue no. 21055) per the manufacturer's instructions.

Statistical Analysis

The results are expressed as means ± S.E. Statistical significance was assessed by Student's unpaired *t* test. Significance was determined as probability (*p*) less than 0.05.

RESULTS

Uncoupled Nitric-oxide Synthase Contributes to Ang II-induced Oxidative Stress in MCs—In pathological states, NOS dysfunction, or "uncoupling," leads to increased generation of superoxide anion by the enzyme associated with a decrease in NO formation (28–30, 34, 35, 41, 46). To delineate the time periods for which NOS is uncoupled, we evaluated the temporal effect of Ang II on both superoxide and NO production. The contribution of uncoupled NOS to ROS production was determined by measuring superoxide generation in the presence and absence of the NOS inhibitor L-NAME (N^G-nitro-L-arginine methyl ester). Intracellular superoxide production was evaluated using DHE (10 μM, 30 min) and confocal microscopy, multiwell fluorescence plate reader, or HPLC. We found that Ang II-induced increase in intracellular superoxide generation was partially inhibited by L-NAME at 1 h and nearly abrogated when MCs were exposed to Ang II for 24 h (Fig. 1, *A–C*). HPLC analysis of the superoxide specific product of DHE, EOH, validated the specificity of superoxide measurements with DHE. These data demonstrate that during these time periods, NOS contributes to Ang II-mediated oxidative stress. The data also indicate that in the early phase (within 10 min), the superoxide generated in response to Ang II is not derived from NOS because superoxide production is insensitive to L-NAME (Fig. 1, *A–C*).

Treatment of MCs with Ang II decreased cGMP production, a reflection of NO bioactivity. The inhibitory effect of Ang II was maximal at 30–60 min and persisted for 24 h (Fig. 2*A*). Similar results were obtained when nitrite formation, the stable end product of NO synthesis, was evaluated (Fig. 2*B*). We also assayed NOS activity in MC lysates by monitoring the conversion of radiolabeled L-arginine to L-citrulline, which is formed stoichiometrically with NO, and yields information on the capacity of NOS to make NO. Consistent with cGMP and nitrite findings, NOS activity was significantly reduced in MCs exposed to Ang II for 1 and 24 h (Fig. 2*C*). These data confirm that NOS generates lesser amount of NO upon stimulation with Ang II, resulting in diminished NO bioavailibility, and further support the idea that Ang II promotes NOS uncoupling in MCs.

eNOS Is Uncoupled upon Exposure of MCs to Ang II and Is a Source of Intracellular ROS—As previously reported (35, 36), we found that eNOS protein is present in MCs (Fig. 3*A*, *left panel*). Glomerular endothelial cells were used as positive control. eNOS expression was also visualized in MCs by immunofluorescence and confocal microscopy (Fig. 3*A*, *right panel*). As shown in Fig. 3*B*, the eNOS protein band expression was markedly decreased after transfection of MCs with specific siRNA oligonucleotides for eNOS (sieNOS), but not nontargeting siRNA (Scr), thereby confirming its identity. Because eNOS is highly expressed in MCs, we tested the hypothesis that eNOS is the NOS isoform uncoupled upon stimulation with Ang II. To this end, we used a siRNA strategy, and DHE fluorescence was assessed. Down-regulation of eNOS protein expression by sieNOS mimicked the effects of L-NAME on Ang II-induced superoxide generation in MCs (compare Fig. 1, *A–C*, and Fig. 3, *C* and *D*). Superoxide production in response to Ang II was partially decreased by sieNOS at 1 h, nearly abolished at 24 h, and not altered at 10 min (Fig. 3, *C* and *D*). These data also validate the assumption that another source, distinct from dysfunctional NOS, contributes to Ang II-induced oxidative stress for the early time points.

Because dimer formation and stability are critical for eNOS to functionally produce NO and are affected in the uncoupled enzyme, we determined the proportion of eNOS existing as either dimer or monomer in MCs treated with Ang II. Electrophoresis of MC lysates without prior heat denaturation (low temperature SDS-PAGE) showed bands approximately twice the size of eNOS monomer, attributable to eNOS dimer. Exposure of the cells to Ang II for 1 or 24 h showed a significant reduction in the dimer to monomer ratio compared with control (Fig. 3, *E* and *F*). The decrease in dimer started at 15–30 min, and maximum decrease was observed at 1 h (Fig. 3*E*). These events occur at time periods for which we found that uncoupled NOS participate to Ang II-mediated superoxide generation and NO production was decreased.

Because they also are susceptible to uncoupling and present in the renal tissue (47), the involvement of the other NOS isoforms (neuronal and inducible) was considered. Fig. 3*G* shows that iNOS and nNOS protein are not expressed in MCs under basal conditions. Short or prolonged exposure of the cells to Ang II did not induce the expression of iNOS or nNOS protein (Fig. 3*G*), indicating that iNOS and nNOS are most likely not involved in the actions of Ang II in MCs. Taken together, these findings indicate that uncoupled eNOS is a source of ROS in MCs treated with Ang II and provide a rationale for studying the mechanism(s) by which the enzyme is uncoupled in these cells.

Uncoupled eNOS Is Required for Ang II-induced Fibronectin Synthesis in MCs—Using MCs as a model to study the mechanism of abnormal matrix accumulation by kidney cells, we have recently shown that Ang II promoted fibronectin expression through a redox-dependent pathway (25, 26). We explored the

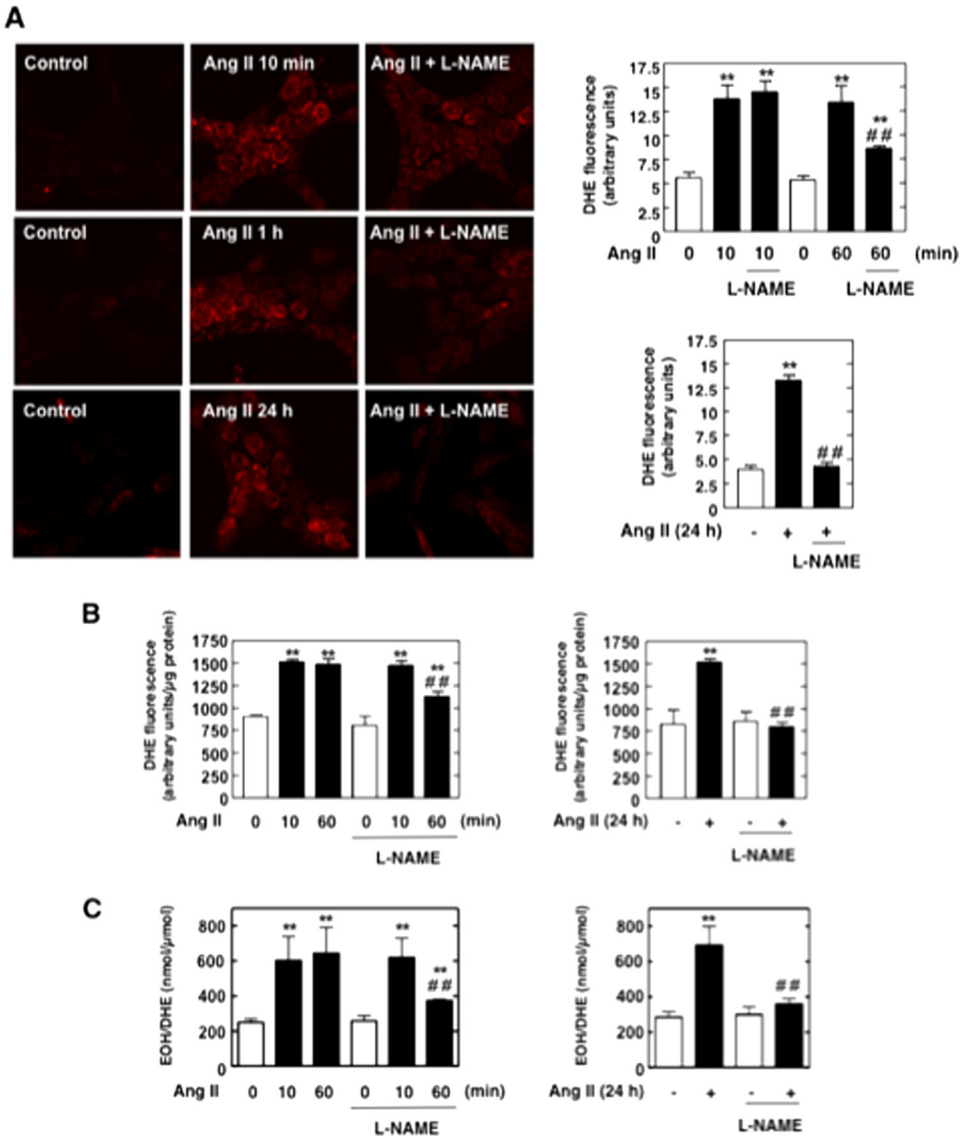

FIGURE 1. **Uncoupled NOS contributes to Ang II-induced intracellular superoxide generation in MCs.** Serum-deprived MCs were preincubated with the NOS inhibitor L-NAME (100 μM, 3 h) before treatment with 1 μM Ang II for 10 min, 1 h, or 24 h. Intracellular superoxide generation was evaluated using DHE (10 μM, 30 min) and confocal microscopy (*A*), DHE and a multiwell fluorescence plate reader (*B*), or DHE and HPLC (*C*) as described under "Experimental Procedures." In *A*, the *right histograms* represent the semiquantification of relative DHE fluorescence (arbitrary units). In *A–C*, the values are the means ± S.E. from three independent experiments. **, $p < 0.01$ *versus* control. ##, $p < 0.01$ *versus* Ang II.

possibility that ROS derived from dysfunctional eNOS mediate the fibrotic response to Ang II in MCs by examining the effects of L-NAME or sieNOS on Ang II-induced fibronectin protein expression. Incubation of MCs with L-NAME or depletion of eNOS protein by specific siRNA, but not nontargeting siRNA, significantly inhibited Ang II-induced increase in fibronectin synthesis as measured by Western blotting (Fig. 4, *A* and *C*) and immunofluorescence (Fig. 4, *B* and *D*). These data indicate that uncoupled eNOS is critical for the chronic action of Ang II on fibronectin synthesis in MCs.

Peroxynitrite Is Implicated in Ang II-induced eNOS Dysfunction/Decline in NO Bioavailability and Fibronectin Expression—Peroxynitrite, the reaction product of NO and superoxide, is a strong oxidant capable of promoting NOS uncoupling through oxidative modification of the enzyme, including oxidation of BH_4 and the zinc cluster (28–30, 34–36, 41, 46). Thus, we hypothesized that peroxynitrite participated to Ang II-mediated eNOS dysfunction in MCs. Ang II caused a rapid increase in 3-nitrotyrosine, a footprint of peroxynitrite production, at 10 and 60 min as assessed by Western blot (Fig. 5*A*), ELISA (Fig. 5*B*), and immunofluorescence analysis (Fig. 5*C*). Importantly, peroxynitrite formation preceded eNOS dysfunction (that take place at 60 min), suggesting that peroxynitrite plays a role in eNOS uncoupling. Preincubation of MCs with the peroxynitrite scavenger uric acid significantly reduced Ang II-induced 3-nitrotyrosine staining, indicating that the signal corresponded to peroxynitrite formation (Fig. 5*D*). In addition, treatment of MCs with L-NAME also markedly inhibited the enhancement of 3-nitrotyrosine staining seen in cells exposed to Ang II for 10 and 60 min (Fig. 5*D*), demonstrating that NOS is required for peroxynitrite production, most likely via providing the required NO. The implication of peroxynitrite in eNOS dysfunction is validated by the observation that preincubation of MCs with uric acid was able to prevent the decline in NO

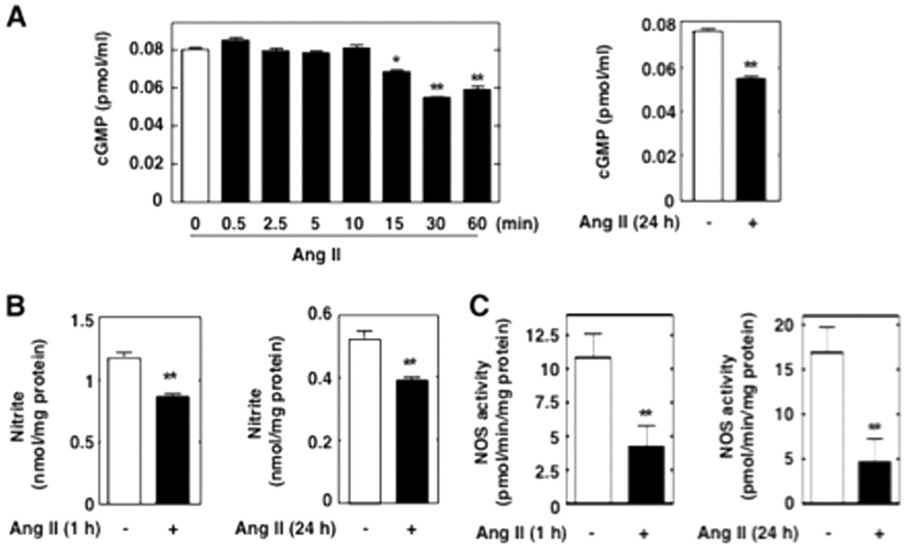

FIGURE 2. **Ang II promotes a decrease in NO bioavailability and inhibition of NOS in MCs.** *A*, treatment of serum-deprived rat MCs with 1 μM Ang II for a short time period (*left panel*) or a prolonged time period (*right panel*) causes a decrease in cGMP synthesis, an indicator of NO bioactivity. The values are the means ± S.E. of three independent experiments. *, $p < 0.05$; **, $p < 0.01$ *versus* control. *B* and *C*, treatment of serum-deprived rat MCs with 1 μM Ang II for 1 or 24 h causes a decrease in nitrite formation, the stable end product of NO synthesis (*B*), and NOS activity (*C*). NOS activity was measured in MC lysate by monitoring the formation of L-[^{14}C]citrulline from L-[^{14}C]arginine. Activity is expressed as pmol citrulline/min/mg protein. The values are the means ± S.E. of three independent experiments. **, $p < 0.01$ *versus* control.

bioavailability triggered by Ang II (Fig. 5*E*) at the time periods for which eNOS is dysfunctional (1 and 24 h). Scavenging of peroxynitrite with uric acid also inhibited Ang II-induced fibronectin accumulation in MCs (Fig. 5*F*). These findings highlight the crucial role of peroxynitrite in eNOS dysfunction, decreased NO levels, and the resulting fibrotic response of MC to Ang II.

The Up-regulation of Nox4 Mediates Ang II-induced Early Increase in Peroxynitrite Generation and eNOS Dysfunction in MCs—The Nox family of NADPH oxidases, in response to various stimuli, produces superoxide that combines with NO to form peroxynitrite capable of uncoupling eNOS and impairing NO bioavailability. Because NADPH oxidase Nox4 is highly expressed and plays a role in Ang II redox signaling in MCs (24–26), we hypothesized that Nox4-derived superoxide was required for the peroxynitrite-dependent alteration of eNOS function and the subsequent decline in NO levels. We found that short exposure of MCs to Ang II up-regulates Nox4 protein expression (Fig. 6*A*) and increased NADPH-dependent superoxide generation (Fig. 6*B*) in the total cell homogenate. The increase in Nox4 protein expression promoted by Ang II was observed as early as 2.5 min and is sustained up to 60 min.

To establish that Nox4 is necessary for Ang II-induced intracellular superoxide production, Nox4 expression was down-regulated with specific siRNA. First, we confirmed that transfection of siRNA for Nox4 (siNox4), but not non-targeting siRNA (Scr), reduces Nox4 protein abundance (Fig. 6*C*). Note that for every RNA interference experiment described in this report, the siRNAs transfected obtained from Dharmacon corresponded to a SMARTpool consisting of four siRNAs specific for the protein of interest. Importantly, siNox4 abolished the increase in NADPH oxidase activity (Fig. 6*D*) and intracellular superoxide caused by Ang II at early time points (Fig. 6, *E* and *F*). In these experiments, superoxide specific product of DHE, 2-ETOH was measured using HPLC-based method (Fig. 6*E*), and DHE fluorescence was visualized with laser-scanning confocal microscopy (Fig. 6*F*). These findings indicate that Nox4 is responsible for the increased generation of intracellular ROS in response to acute treatment of MCs with Ang II and that this increase is most likely due to an acute up-regulation of Nox4 protein expression. Together with the observations reported in Figs. 1 and 3, these data suggest that in the early phase (within 10 min) the superoxide generated in response to Ang II may be derived from Nox4 but not NOS, whereas at later time point (60 min) both NOS and Nox4 contribute to superoxide generation.

We also found that siRNA-mediated inhibition of Nox4 markedly reduced Ang II-induced early increase in 3-nitrotyrosine as measured by ELISA (Fig. 7*A*) and immunofluorescence analysis (Fig. 7*B*), indicating that Nox4 is required for peroxynitrite generation. Fig. 7*C* establishes the functional link between Nox4 and the alteration of NO bioavailibility. Indeed, impairment of Nox4 function with specific siRNA, but not non-targeting siRNA, prevented Ang II-induced decrease in NO levels at 1 or 24 h (the time points where eNOS is uncoupled) (Fig. 7*C*). Fig. 7*D* confirmed the effective down-regulation of Nox4 protein with siRNA in these cells. Nox4 appears to act as a critical mediator of eNOS dysfunction and decrease in NO bioavailability in these cells. These data strongly suggest that Nox4-derived superoxide reacts with NO generated constitutively by coupled eNOS, resulting in the formation of peroxynitrite that subsequently alters eNOS function and NO bioavailability.

Mitochondrial Nox4 Is Up-regulated by Ang II and Contributes to Ang II-dependent Superoxide Generation in MCs—We have previously shown that a functional and active Nox4 is present in mitochondria from MCs (21). Therefore, we examined whether Nox4 is involved in Ang II-induced ROS genera-

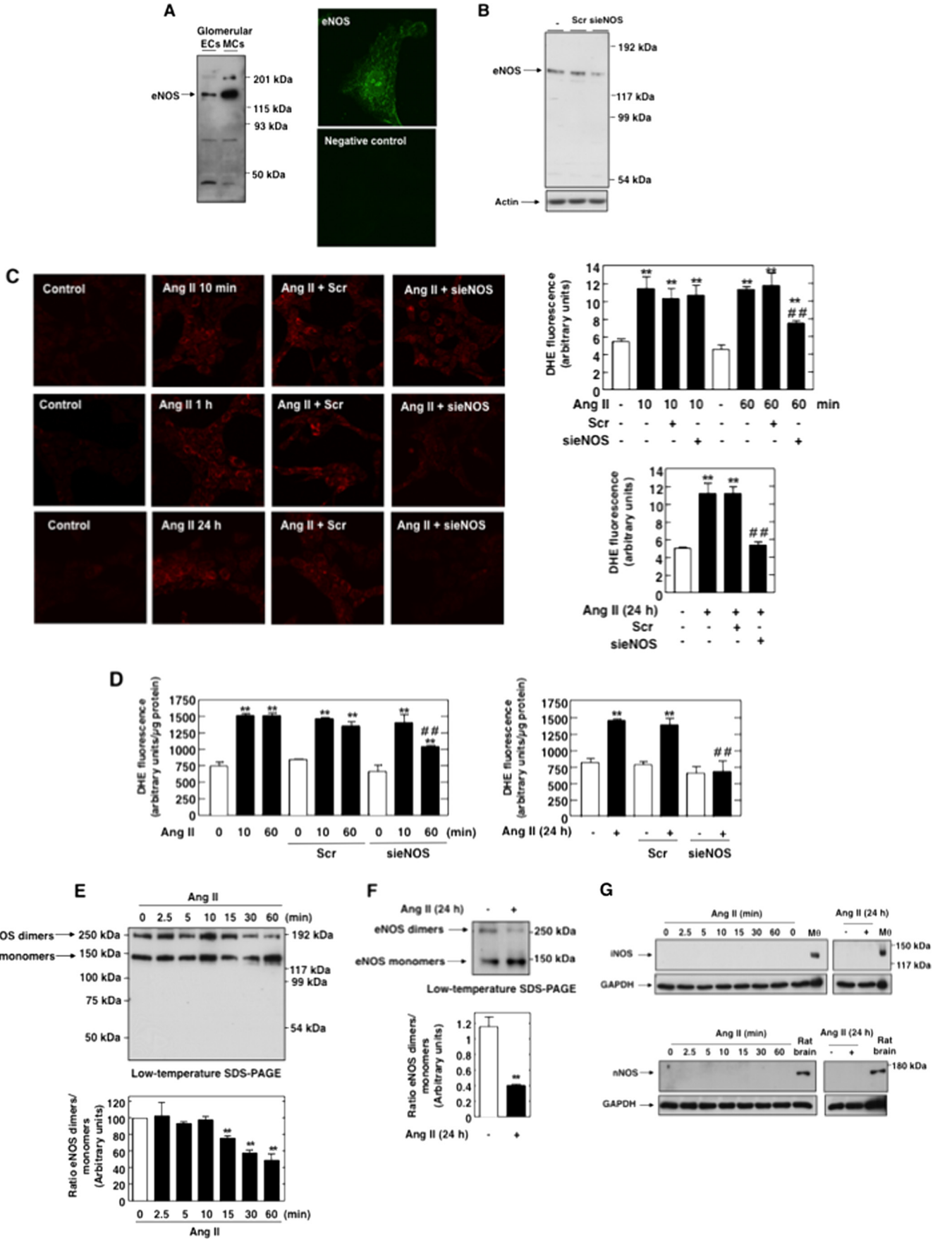
A
Glomerular
ECs MCs
eNOS
201 kDa
115 kDa
93 kDa
50 kDa
eNOS
Negative control
B
Scr sieNOS
eNOS
192 kDa
117 kDa
99 kDa
54 kDa
Actin
C
Control
Ang II 10 min
Ang II + Scr
Ang II + sieNOS
Control
Ang II 1 h
Ang II + Scr
Ang II + sieNOS
Control
Ang II 24 h
Ang II + Scr
Ang II + sieNOS
DHE fluorescence (arbitrary units)
Ang II - 10 10 10 - 60 60 60 min
Scr - - + - - - + -
sieNOS - - - + - - - +
DHE fluorescence (arbitrary units)
Ang II (24 h) - + + +
Scr - - + -
sieNOS - - - +
D
DHE fluorescence (arbitrary units/μg protein)
Ang II 0 10 60 0 10 60 0 10 60 (min)
Scr
sieNOS
DHE fluorescence (arbitrary units/μg protein)
Ang II (24 h) - + - + - +
Scr
sieNOS
E
Ang II
0 2.5 5 10 15 30 60 (min)
eNOS dimers
eNOS monomers
250 kDa
150 kDa
100 kDa
75 kDa
50 kDa
192 kDa
117 kDa
99 kDa
54 kDa
Low-temperature SDS-PAGE
Ratio eNOS dimers/ monomers (Arbitrary units)
0 2.5 5 10 15 30 60 (min)
Ang II
F
Ang II (24 h) - +
eNOS dimers
eNOS monomers
250 kDa
150 kDa
Low-temperature SDS-PAGE
Ratio eNOS dimers/ monomers (Arbitrary units)
Ang II (24 h) - +
G
Ang II (min)
0 2.5 5 10 15 30 60 0 MΘ
Ang II (24 h)
- + MΘ
iNOS
GAPDH
150 kDa
117 kDa
Ang II (min)
0 2.5 5 10 15 30 60
Rat brain
Ang II (24 h)
- +
Rat brain
nNOS
GAPDH
180 kDa

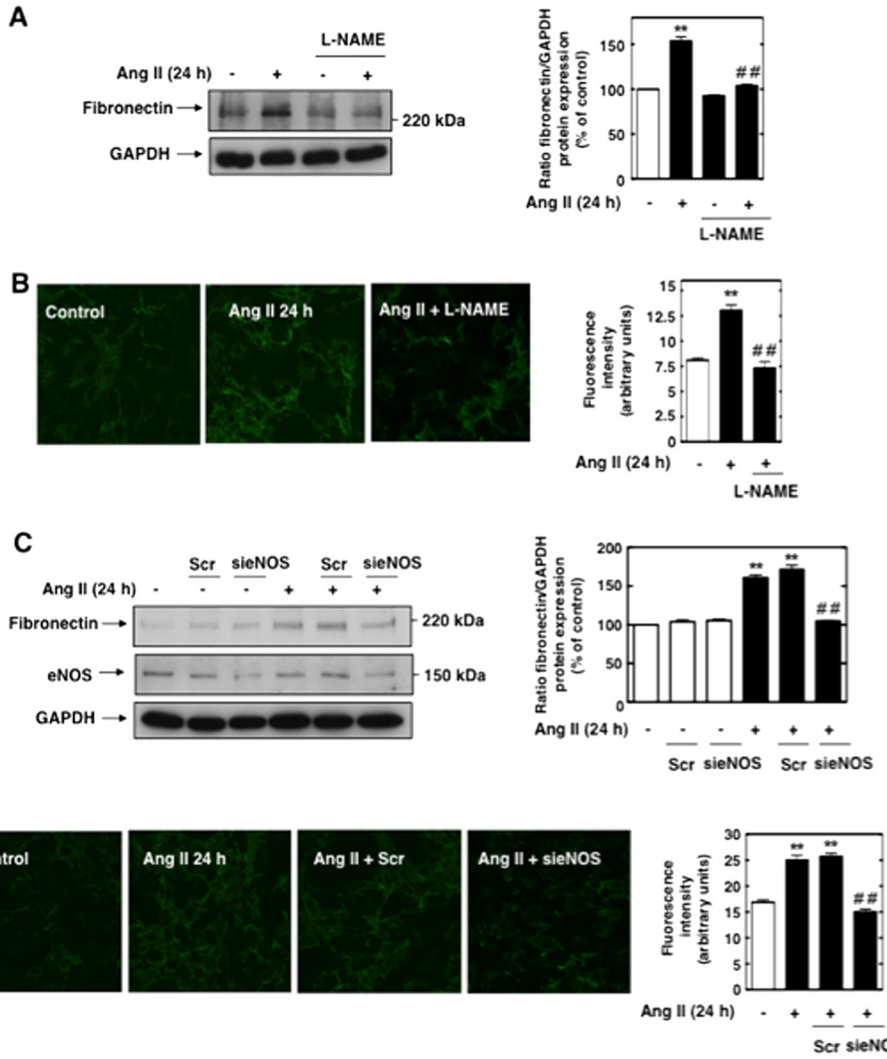

FIGURE 4. **Uncoupled eNOS contributes to Ang II-induced fibronectin accumulation in MCs.** *A* and *B*, serum-deprived MCs were preincubated with the NOS inhibitor L-NAME (100 μM, 3 h) before treatment with Ang II (1 μM) for 24 h, and fibronectin deposition was evaluated by direct immunoblotting of cell lysates (*A*) or by immunofluorescence with confocal microscope (*B*). *C* and *D*, MCs were untransfected, transfected with 100 nM Scr or sieNOS, and exposed or not to Ang II (1 μM) for 24 h. Fibronectin protein expression was determined by direct immunoblotting of cell lysates (*C*) or by immunofluorescence and confocal microscopy (*D*). In *C*, the knockdown of eNOS protein by siRNA is shown in the *middle panel*. In *A* and *C*, *right panels*, histograms representing the ratio of the intensity of fibronectin bands quantified by densitometry factored by the densitometric measurement of GAPDH band. The data are expressed as percentages of control (untreated or untransfected cells), where the ratio in the control was defined as 100%. The values are the means ± S.E. from three independent experiments. In *B* and *D*, *right panels*, histograms represent the semiquantification of fluorescence intensity. The photomicrographs are representative of three individual experiments. **, $p < 0.01$ *versus* control. ##, $p < 0.01$ *versus* HG in untreated or untransfected cells.

tion in MCs. Mitochondria were isolated by using a mitochondria fractionation kit that allowed the fractionation of MCs into cytosol and Mit (Fig. 8*A*). As expected, Nox4 localized to mitochondria, but not to cytosol (Fig. 8*A*). The mitochondrial, but not cytosolic, fraction was positive for the mitochondria-specific protein prohibitin (Fig. 8*A*). Note that eNOS was not found in the mitochondrial fraction (Fig. 8*A*). Immunofluorescence confocal microscopy was also used to localize Nox4 in MCs by

FIGURE 3. **Uncoupled eNOS contributes to Ang II-induced intracellular superoxide generation in MCs.** *A*, eNOS is expressed in glomerular MCs. *Left panel*, immunoblot detection using anti-eNOS antibodies shows a 130–145-kDa band corresponding to the predicted molecular weight of the enzyme in glomerular endothelial cells and MCs. *Right panel*, immunofluorescence confocal microscopy using eNOS antibody and FITC-linked secondary antibodies showing eNOS distribution in MCs. *B*, MCs were untransfected (−) and transfected with control Scr (100 nM) or with sieNOS (100 nM). eNOS protein expression was determined by Western blot analysis. Transfection of MCs with sieNOS but not Scr reduces the 130–145-kDa band. *C* and *D*, MCs were untransfected or transfected with Scr or sieNOS and exposed to 1 μM Ang II for 10 min, 1 h, or 24 h. Intracellular superoxide generation was evaluated using DHE (10 μM, 30 min) and confocal microscopy (*C*) or DHE and a multiwell fluorescence plate reader (*D*) as described under "Experimental Procedures." In *C*, the *right panels* represent a semiquantification of relative DHE fluorescence (arbitrary units). The values are the means ± S.E. from three independent experiments. **, $p < 0.01$ *versus* control. ##, $p < 0.01$ *versus* Ang II in untransfected cells. *E* and *F*, Ang II decrease the eNOS dimer to monomer ratio, a reflection of the disruption of eNOS dimer stability and eNOS uncoupling. Serum-deprived MCs were exposed to 1 μM Ang II for the indicated times, and samples were subjected to low temperature SDS-PAGE. The Western blots shown are representative of at least three independent experiments. The *bottom panels* represent the ratio of the intensity of eNOS dimer bands quantified by densitometry factored by the densitometric measurement of eNOS monomer band. The values are the means ± S.E. from three independent experiments. **, $p < 0.01$ *versus* control. *G*, treatment of the cells with Ang II (1 μM) for short or prolonged time periods did not increase the expression of iNOS or nNOS protein. Serum-deprived MCs were exposed to 1 μM Ang II for a short or prolonged time period. iNOS (*top panel*) or nNOS (*bottom panel*) proteins were determined by direct immunoblotting. *Mθ*, LPS-activated macrophage lysate used as positive control for iNOS. Rat brain was used as a positive control for nNOS.

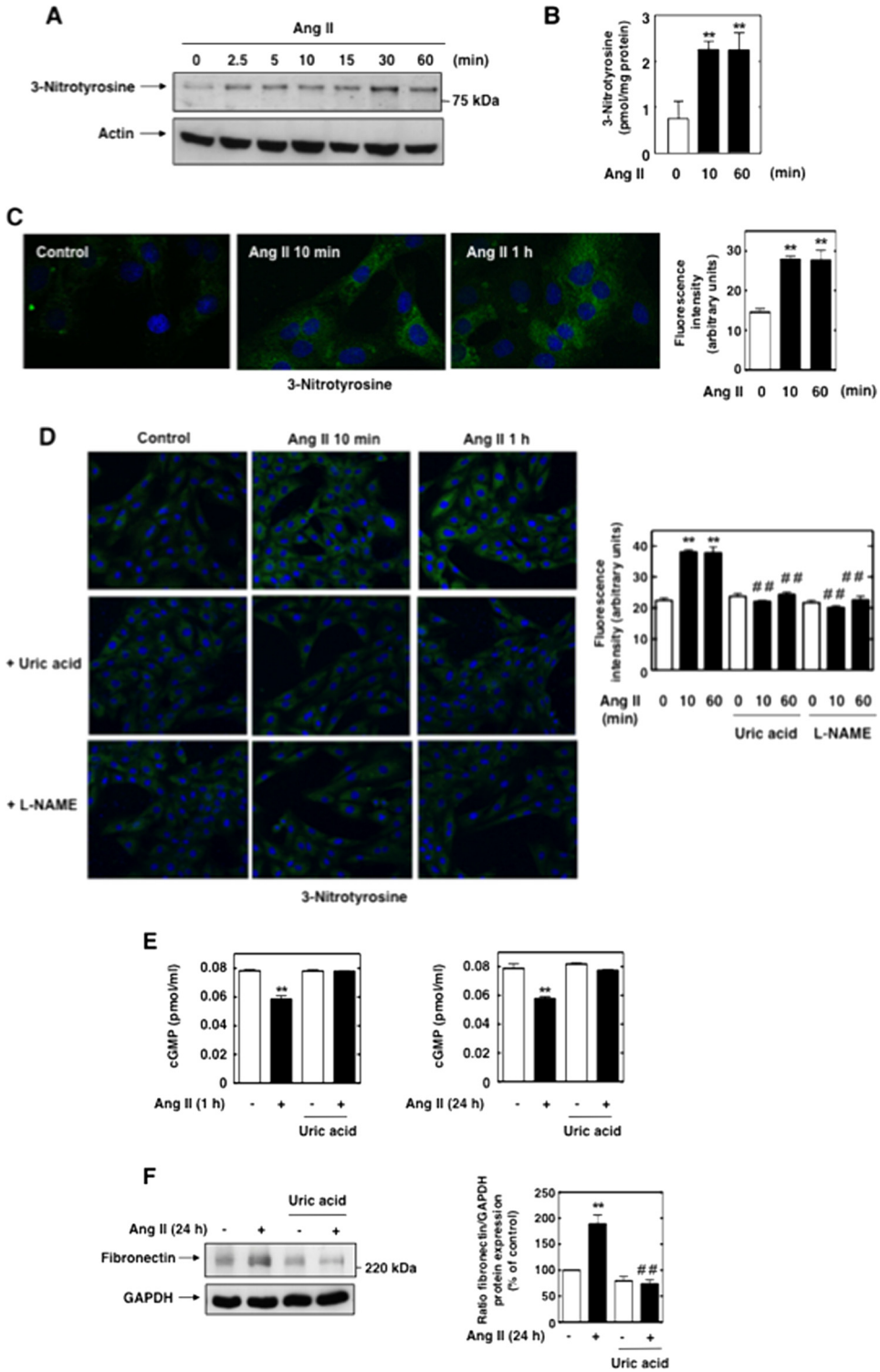

FIGURE 5. **Peroxynitrite is required for eNOS uncoupling and the expression of fibronectin in response to Ang II.** *A* and *B*, Ang II causes a rapid increase in 3-nitrotyrosine, a footprint of peroxynitrite generation. Serum-deprived MCs were treated with 1 μM Ang II for the indicated time, and 3-nitrotyrosine levels were assessed using Western blot analysis (*A*), an enzyme immunoassay kit (*B*), or immunofluorescence and confocal laser microscopy (*C*). *C*, *right panel*, semiquantification of fluorescence intensity. The values are the means ± S.E. from three independent experiments. **, $p < 0.01$ *versus* control. *D*, serum-deprived MCs were pretreated with uric acid (200 μM, 3 h), a peroxynitrite scavenger, or L-NAME (100 μM, 3 h) before exposure to Ang II (1 μM) for 10 min or 1 h, and 3-nitrotyrosine was evaluated by immunofluorescence staining. *Right panel*, semiquantification of fluorescence intensity. The values are the means ± S.E. from three independent experiments. **, $p < 0.01$ *versus* control. ##, $p < 0.01$ *versus* HG. *E*, serum-deprived MCs were pretreated with uric acid (200 μM, 3 h) before exposure to Ang II for 1 or 24 h, and NO bioactivity was assessed by measuring cGMP synthesis. The values are the means ± S.E. from three independent experiments. **, $p < 0.01$ *versus* control. *F*, serum-deprived MCs were pretreated with uric acid (200 μM, 3 h) before exposure to Ang II for 24 h, and fibronectin protein expression was determined by direct immunoblotting of cell lysates. *Right panel*, histogram representing the ratio of the intensity of fibronectin bands quantified by densitometry factored by the densitometric measurement of GAPDH bands. The data are expressed as in Fig. 4. The values are the means ± S.E. from three independent experiments. **, $p < 0.01$ *versus* control. ##, $p < 0.01$ *versus* Ang II in untreated cells.

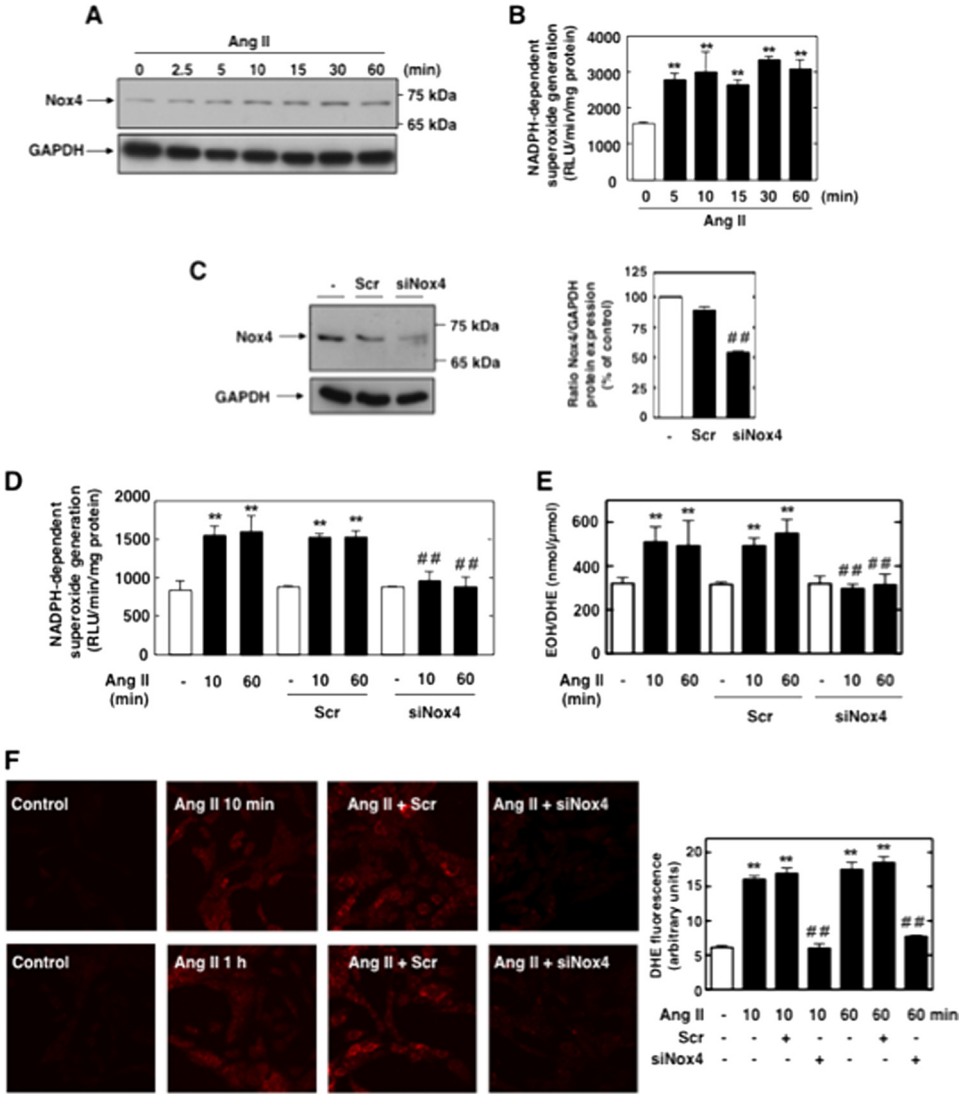

FIGURE 6. **Nox4 is up-regulated by Ang II and mediates Ang II-induced acute intracellular ROS production in MCs.** *A*, serum-starved MCs were treated for the indicated time with Ang II (1 μM), and Nox4 protein expression was evaluated by Western blot analysis in whole cell homogenate. *B*, serum-starved MCs were stimulated with 1 μM Ang II for the indicated time periods, and NADPH-dependent superoxide generation was measured by the lucigenin (5 μM)-enhanced chemiluminescence method in MC homogenates. The initial rate of enzyme activity was calculated and expressed as relative chemiluminescence (light) units (*RLU*)/min/mg protein as described under "Experimental Procedures." The values are the means ± S.E. of three independent experiments. **, $p <$ 0.01 *versus* control. *C*, MCs were untransfected (−) or transfected with Scr or siNox4. Nox4 protein knockdown with siNox4, but not Scr, was confirmed by Western blot analysis. *Right*, histogram representing the ratio of the intensity of Nox4 bands quantified by densitometry factored by the densitometric measurement of GAPDH bands. The data are expressed as percentages of control, where the ratio in the control was defined as 100%. **, $p <$ 0.01 *versus* control. ##, $p <$ 0.01 *versus* untransfected cells. *D–E*, MCs were untransfected, transfected with Scr or siNox4, and exposed or not to Ang II (1 μM) for 10 min or 1 h. ROS generation was then assessed by measuring NADPH oxidase activity in MC homogenates (*D*) and DHE fluorescence with HPLC (*E*) or confocal microscope (*F*). In *F*, the *right panel* represents the semiquantification of fluorescence intensity. The values are the means ± S.E. from three independent experiments. **, $p <$ 0.01 *versus* control. ##, $p <$ 0.01 *versus* Ang II in untransfected cells.

using FITC-conjugated anti-rabbit IgG. As shown in Fig. 8*B*, Nox4 colocalizes with the mitochondrial marker Mitotracker Deep Red 633. Importantly, treatment of MCs with Ang II for 10 min or 1 h promotes an increase in Nox4 protein expression in the mitochondrial fraction as assessed by Western blot analysis (Fig. 8*C*). Transfection of MCs with siNox4 resulted in down-regulation of the 70–75-kDa band detected by immunoblot analysis in the mitochondrial fraction, thereby validating that this band corresponds to Nox4 protein (Fig. 8*D*, *left panel*). Similarly, immunofluorescence studies showed that the mitochondrial staining pattern of Nox4 is strongly diminished (Fig. 8*D*, *right panel*). Studies using MitoSOX Red, a fluorogenic dye detecting selectively mitochondrial superoxide, showed that MitoSOX fluorescence is increased after acute exposure of MCs to Ang II (10 min or 1 h) (Fig. 8, *E* and *F*). Of interest is that Ang II-stimulated mitochondrial superoxide generation colocalizes with Nox4. Note also that immunofluorescence studies confirmed the up-regulation of Nox4 by Ang II in mitochondria. Down-regulation of Nox4 by transfection of the cells with siNox4, but not Scr, prevented the Ang II-induced increase in mitochondrial superoxide assessed by MitoSOX Red (Fig. 8, *E* and *F*). These findings indicate that mitochondrial Nox4 is rapidly up-regulated by Ang II and participates in the rapid generation of ROS induced by the hormone.

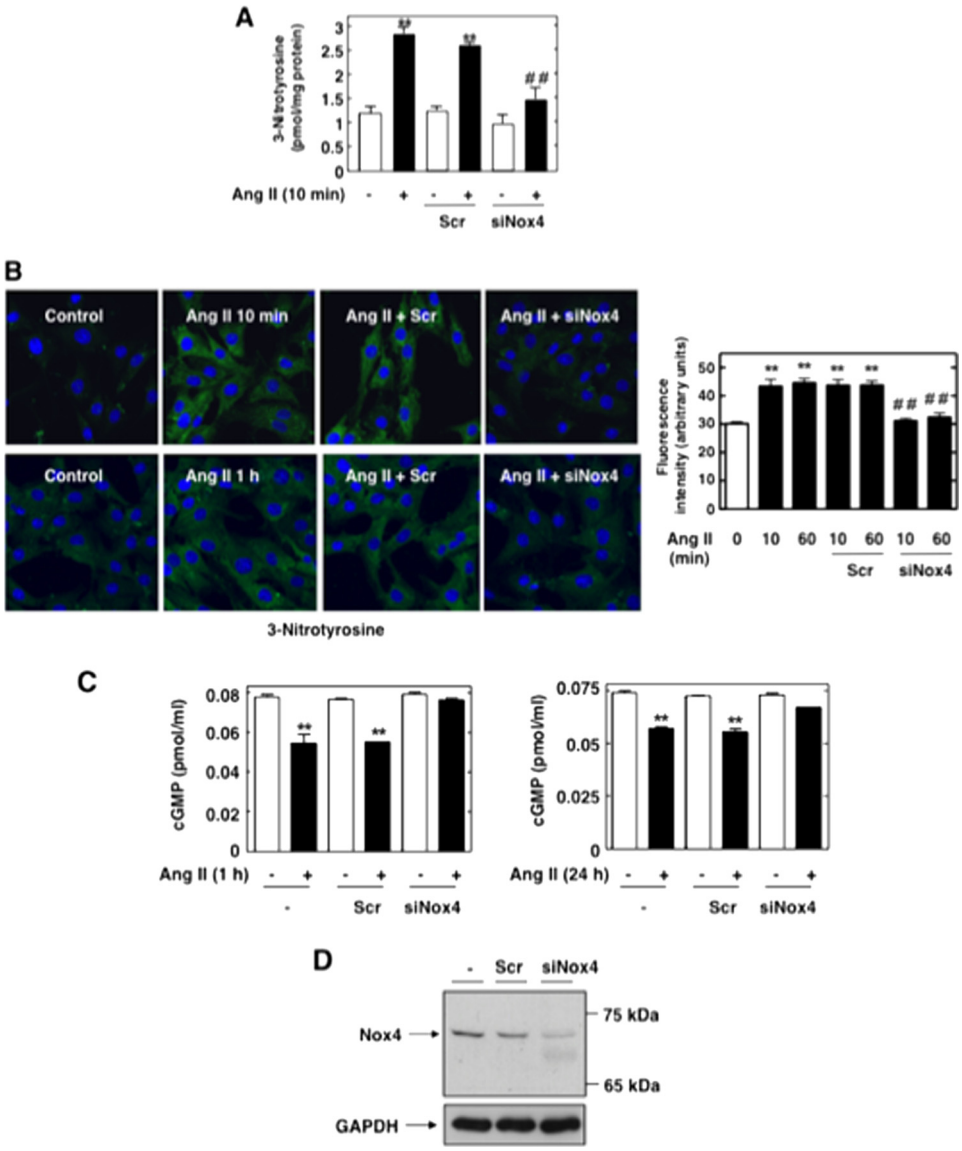

FIGURE 7. **Nox4 mediates Ang II-induced early increase in peroxynitrite generation and eNOS dysfunction in MCs.** *A* and *B*, serum-deprived MCs transfected with Scr or siNox4 were treated with or without μM Ang II for 10 min or 1 h, and 3-nitrotyrosine was assessed with an enzyme immunoassay kit (*A*) and immunofluorescence with confocal laser microscopy (*B*). In *B*, the *right panel* represents the semiquantification of fluorescence intensity. The values are the means ± S.E. from three independent experiments. **, $p < 0.01$ *versus* control; ##, $p < 0.01$ *versus* Ang II in untransfected cells. *C*, serum-deprived MCs untransfected or transfected with Scr or siNox4 were treated with or without Ang II (1 μM) for 1 h or 24 h, and cGMP synthesis was assessed. The values are the means ± S.E. from three independent experiments. **, $p < 0.01$ *versus* control. *D*, MCs were untransfected or transfected with nontargeting Scr or with siNox4, and Nox4 protein expression was determined by Western blot analysis.

Mitochondrial Superoxide Is Involved in Ang II-induced eNOS Dysfunction/Decrease in NO Bioavailability and Fibrotic Response in MCs—In an attempt to connect Nox4-dependent increase in mitochondrial superoxide stimulated by Ang II to eNOS uncoupling/decline in NO levels and abnormal extracellular matrix protein, MnSOD, the mitochondrial form of SOD, was overexpressed in MCs. Infection of MCs with AdMnSOD increased its protein expression in total cell lysate and Mit fraction as assessed by Western blot analysis (Fig. 9*A*). AdβGal was used as control. Overexpression of MnSOD in MCs abolished Ang II-induced acute increase in mitochondrial superoxide generation as reflected by MitoSOX fluorescence (Fig. 9*B*). This indicates that MnSOD effectively affects mitochondrial superoxide and also that MitoSOX is a valid probe for the visualization of the superoxide produced in mitochondria. The observation that AdMnSOD mimics the effect of Nox4 siRNAs on the stimulation of mitochondrial superoxide production by Ang II (both abolished MitoSOX signal) suggests that the effects of AdMnSOD may be due to degradation of Nox4-derived superoxide. AdMnSOD significantly reduced the enhancement of peroxynitrite generation observed after treatment of MCs with Ang II for 10 min and 1 h (Fig. 9*C*), suggesting that mitochondrial ROS are required for the production of the peroxynitrite that initiate eNOS uncoupling. Moreover, removal of mitochondrial superoxide by expression of MnSOD completely prevented the decline in NO caused by Ang II at 1 and 24 h, indicating that mitochondrial superoxide plays a key role in Ang II-mediated eNOS dysfunction (Fig. 9*D*). Additionally, we showed that infection of MCs with AdMnSOD significantly reduced Ang II-induced fibronectin expression by Western

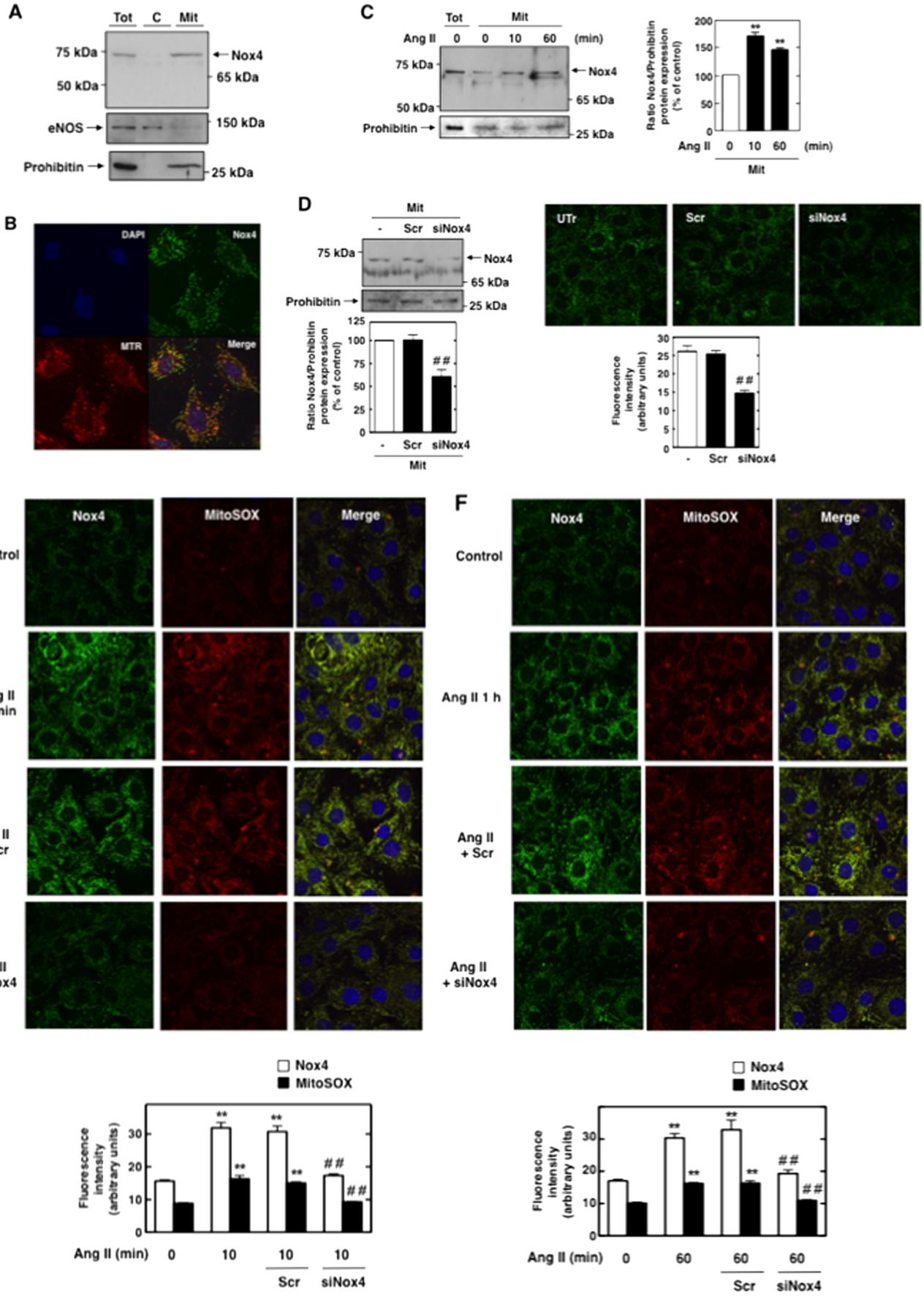
A
Tot
C
Mit
75 kDa
50 kDa
Nox4
65 kDa
eNOS
150 kDa
Prohibitin
25 kDa
B
DAPI
Nox4
MTR
Merge
C
Tot
Mit
Ang II 0 0 10 60 (min)
75 kDa
Nox4
65 kDa
50 kDa
Prohibitin
25 kDa
Ratio Nox4/Prohibitin protein expression (% of control)
200
150
100
50
0
**
**
Ang II 0 10 60 (min)
Mit
D
Mit
- Scr siNox4
75 kDa
Nox4
65 kDa
Prohibitin
25 kDa
Ratio Nox4/Prohibitin protein expression (% of control)
125
100
75
50
25
0
##
- Scr siNox4
Mit
UTr
Scr
siNox4
Fluorescence intensity (arbitrary units)
30
25
20
15
10
5
0
##
- Scr siNox4
E
Nox4
MitoSOX
Merge
Control
Ang II 10 min
Ang II + Scr
Ang II + siNox4
F
Nox4
MitoSOX
Merge
Control
Ang II 1 h
Ang II + Scr
Ang II + siNox4
Nox4
MitoSOX
Fluorescence intensity (arbitrary units)
30
20
10
0
**
**
**
**
##
##
Ang II (min) 0 10 10 10
Scr siNox4
Nox4
MitoSOX
Fluorescence intensity (arbitrary units)
30
20
10
0
**
**
**
**
##
##
Ang II (min) 0 60 60 60
Scr siNox4

blot (Fig. 9*E*) and immunofluorescence (Fig. 9*F*) analyses. In contrast to MnSOD overexpression, suppression of MnSOD expression with siRNA (Fig. 10*A*) significantly enhanced both basal and Ang II-induced mitochondrial ROS production (Fig. 10*B*), decrease in NO levels (Fig. 10*C*), and fibronectin accumulation (Fig. 10, *D* and *E*). This confirmed that modulation of mitochondrial superoxide by changing MnSOD levels affects NO bioavailability and fibronectin accumulation. Together, these data demonstrate that mitochondrial superoxide is critical for Ang II-stimulated peroxynitrite-dependent eNOS dysfunction and subsequent enhancement in fibronectin synthesis in MCs.

DISCUSSION

eNOS is expressed in MCs and becomes dysfunctional under certain conditions such as diabetes (34–36). However, eNOS contribution to Ang II-induced ROS generation and cell injury has not been investigated. Here, we demonstrate for the first time that uncoupled eNOS contributes to Ang II-induced fibronectin expression and provide new insights concerning the molecular mechanism involved in the fibrotic events triggered by Ang II (Fig. 11). The results show that dysfunctional eNOS contributes relatively early to ROS production and decreased NO bioactivity in Ang II-treated MCs and becomes the predominant source of superoxide implicated in fibronectin accumulation after prolonged exposure of the cells to Ang II. Using peroxynitrite scavenger uric acid, we identified acute peroxynitrite production as an initiator of Ang II-mediated eNOS dysfunction/NO deficiency and the subsequent MC fibrotic response. Peroxynitrite is known to alter eNOS function via oxidation of BH_4, thereby reducing its availability to eNOS (27–30). The possibility of eNOS dysfunction via alteration of BH_4 levels is supported by reports showing that BH_4 supplementation restores NO levels and eNOS function in MCs exposed to high glucose or in glomeruli of diabetic rats (35, 48). Moreover, angiotensin receptor blockade reverses eNOS uncoupling by increasing BH_4 levels in glomeruli from diabetic rats (36). Peroxynitrite elicits eNOS dysfunction by inducing the oxidation of the zinc-thiolate cluster present at the dimer interface in the enzyme, resulting in zinc release and destabilization of eNOS dimers (27–29, 41, 46). Our finding that eNOS dimers are dissociated into monomers by low temperature SDS-PAGE in MCs incubated with Ang II further implicates peroxynitrite-dependent zinc thiolate alteration in eNOS uncoupling.

The Nox family of NADPH oxidases are major sources of ROS implicated in the production of the superoxide that combines with NO to form peroxynitrite responsible for eNOS uncoupling and impairment of NO bioavailability (27–30, 49). In the current study, we propose that Nox4-dependent peroxynitrite generation may act as a potent stimulus for eNOS-derived superoxide production. The data establish a role for the superoxide produced by Nox4 in the formation of peroxynitrite that initiates eNOS dysfunction and decrease in NO levels in cells treated with Ang II. The NO required for peroxynitrite production in this early phase is likely provided by constitutively active eNOS as evidenced by the observation that L-NAME inhibits Ang II-induced 3-nitrotyrosine formation. However, the fact that Nox4 produces more hydrogen peroxide than superoxide compared with other Nox oxidases (12, 50–54) cannot be ignored. As a consequence, because hydrogen peroxide, unlike superoxide, does not react with NO, Nox4 is generally considered to be unlikely to significantly contribute to peroxynitrite generation and NOS uncoupling (51, 53–56). This is reinforced by the recent observations that Nox4-derived hydrogen peroxide enhances eNOS activity and NO signaling. For this reason, the Nox oxidases that have been linked to eNOS uncoupling in vascular pathology are the superoxide-generating homologues Nox1 and Nox2 (57–60). These considerations are mitigated by the numerous studies in cardiac, vascular, or renal cells and tissue demonstrating that Nox4 produces detectable amount of superoxide (20, 21, 40, 61–63). Importantly, several of these reports measured superoxide generation using a DHE- and HPLC-based assay as in the present work or via electron paramagnetic/spin resonance, "gold standards" for superoxide measurement (61–63). Therefore, even if Nox4 produces less superoxide than hydrogen peroxide, it is plausible that the readily diffusible and membrane-permeable NO is still able to react with these moderate amounts of superoxide to form the peroxynitrite required for the initiation of NOS uncoupling.

In the present study, the observations that overexpression of mitochondrial MnSOD in MCs prevented Ang II-induced mitochondrial superoxide production, peroxynitrite formation, loss of NO, and increase in fibronectin accumulation support the idea that mitochondrial superoxide is essential for MC injury. The observation that AdMnSOD inhibits Ang II-induced increase in 3-nitrotyrosine staining at the time periods

FIGURE 8. **Mitochondrial Nox4 is up-regulated by Ang II and mediates Ang II-induced acute ROS production in MC mitochondria.** *A*, Mit were isolated by using a mitochondria purification kit (Pierce). Nox4 protein, eNOS, or mitochondrial marker prohibitin was detected by Western blot analysis. *C*, cytosolic fraction; *Tot*, total cell homogenate. *B*, MC mitochondria were visualized with Mitotracker Red and then stained with Nox4 antibody by using a FITC-linked donkey anti-rabbit secondary antibody. Nuclei were counterstained with DAPI. *C*, serum-deprived MCs were treated with or without 1 μM Ang II for 10 min or 1 h, and Mit were isolated by using a mitochondria purification kit (Pierce). Nox4 protein or the mitochondrial marker prohibitin was detected by Western blot analysis. *Tot*, total cell homogenate. *Right*, histogram representing the ratio of the intensity of Nox4 bands quantified by densitometry factored by the densitometric measurement of GAPDH bands. The data are expressed as percentages of control, where the ratio in the control was defined as 100%. **, $p < 0.01$ *versus* control. *D*, MCs were untransfected (−) or transfected with Scr or siNox4, and Mit were isolated by using a mitochondria purification kit (Pierce). The knockdown of mitochondrial Nox4 protein with siNox4, but not Scr, was confirmed by Western blot (*left*) and immunofluorescence analyses (*right*). *Left*, the *bottom histogram* represents the ratio of the intensity of Nox4 bands quantified by densitometry factored by the densitometric measurement of GAPDH bands. The data are expressed as percentages of control, where the ratio in the control was defined as 100%. *Right*, the *bottom histogram* represents the semiquantification of fluorescence intensity. ##, $p < 0.01$ *versus* untransfected cells. *E* and *F*, representative images obtained by confocal fluorescence microscopy of MitoSOX Red fluorescence in untransfected (control), Scr-transfected, and siNox4-transfected MCs after exposure or not to Ang II (1 μM) for 10 min (*E*) or 1 h (*F*). After fixation and permeabilization, the cells were stained with Nox4 antibody and appropriate FITC-conjugated secondary antibody. Nuclei were counterstained with DAPI. In *E* and *F*, *bottom histograms* represent semiquantification of the fluorescence intensity. The values are the means ± S.E. from three independent experiments. **, $p < 0.01$ *versus* untransfected control. ##, $p < 0.01$ *versus* Ang II in untransfected cells.

that precede or correspond to eNOS uncoupling suggests that mitochondrial ROS contribute to the formation of the peroxynitrite initiating eNOS dysfunction. The role of mitochondrial superoxide is validated by the observation that MnSOD depletion affects NO levels and fibronectin accumulation basally or in the presence of Ang II. We have previously described localization of Nox4 to mitochondria in MCs and that NADPH-dependent superoxide production measured in intact Percoll-purified mitochondria was significantly reduced after Nox4 knockdown, indicating that the enzyme is functional (21). Here, we show that Ang II elicits a rapid increase in mitochondrial superoxide that correlates with the up-regulation of

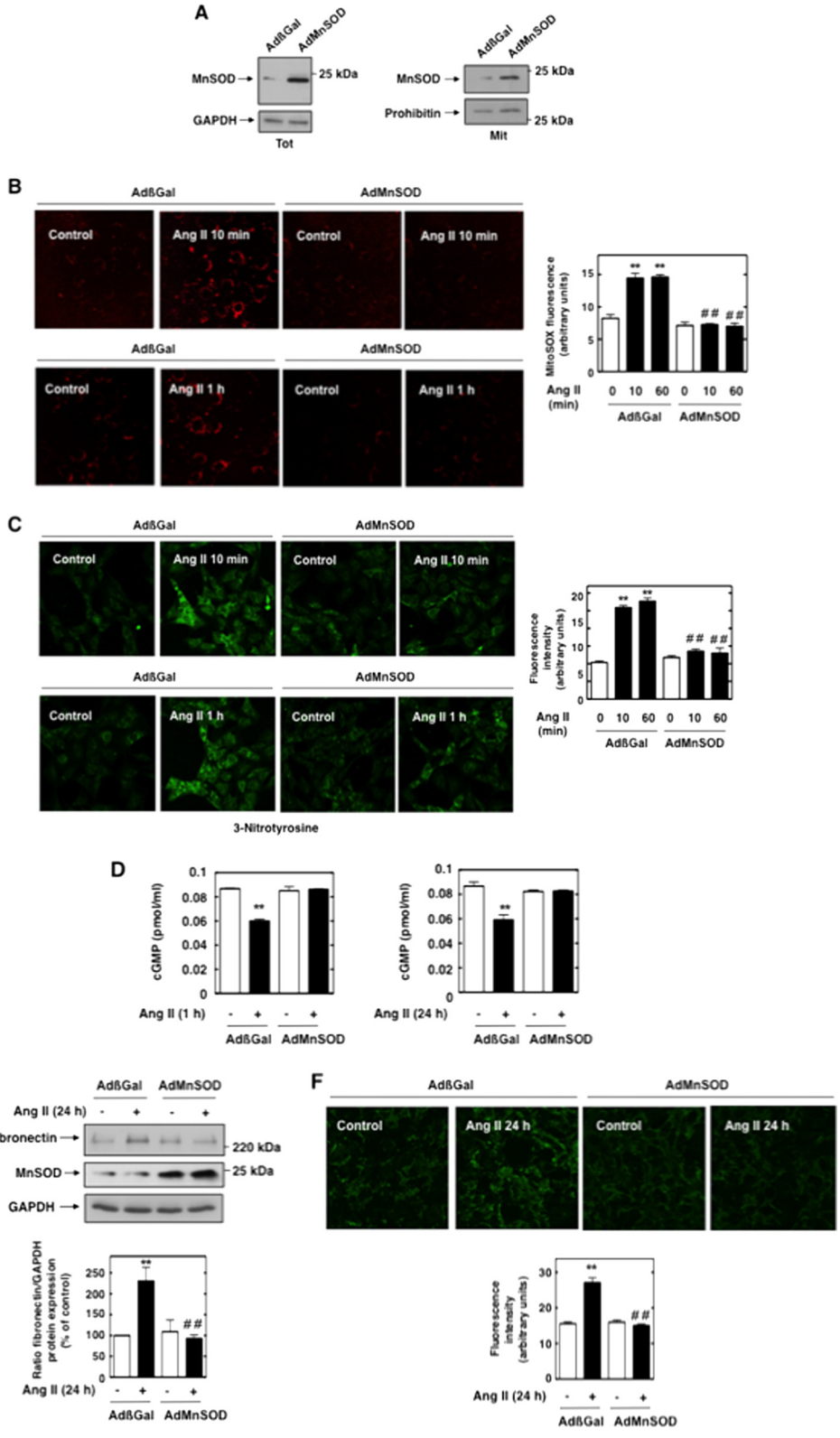

Nox4 protein in the mitochondrial fraction. Down-regulation of cellular and mitochondrial Nox4 with siRNA prevents Ang II-induced increase in mitochondrial superoxide production, identifying Nox4 as a prominent source of mitochondrial ROS in MCs treated with Ang II. These data are in agreement with the recent findings showing that high glucose and Ang II enhance mitochondrial Nox4 expression and the subsequent increase in ROS generation in renal cells (21–23).

Importantly, the fact that Nox4 contributes to mitochondrial ROS generation does not necessarily imply that the oxidase is in the mitochondria because interplay between mitochondria and Nox enzymes located outside the organelles have been described. We have previously reported that Nox4 is also present in MC membranes (21). The siRNAs for Nox4 most likely target both "membrane" and mitochondrial Nox4 and thereby do not allow delineation the role of mitochondrial and non-mitochondrial Nox4 in eNOS uncoupling and subsequent fibronectin expression (Fig. 11). A role for the electron transport chain (ETC) (17–19, 64–67) as a source of mitochondrial superoxide cannot be excluded. A short paracrine loop may exist, by which ROS production by mitochondrial and/or non-mitochondrial Nox4 regulates or is regulated by ROS generation by the mitochondrial respiratory chain (Fig. 11). However, the similarities between the inhibitory effects of Nox4 siRNA and AdMnSOD on Ang II-mediated eNOS dysfunction or fibronectin expression strongly suggest that superoxide generated by Nox4 in mitochondria contributes to the deleterious effects of Ang II in MCs.

The finding that MnSOD, known to operate in the matrix, affects the increase in mitochondrial superoxide promoted by Ang II together with the fact that the superoxide is visualized with MitoSOX, a probe that primarily detect matrix superoxide, suggest that superoxide generation occurs in the matrix. Given the extreme compartmentalization of the mitochondria and the limited ability of superoxide to diffuse through membranes (68, 69), this raises the question of how the superoxide produced in the matrix contributes to the eNOS dysfunction and fibronectin accumulation that occur outside of the mitochondria.

Because NO is a neutral, hydrophobic, diffusible molecule, it is likely that it can easily cross the mitochondrial membranes (68, 70, 71) and react with the superoxide produced in the matrix to form peroxynitrite. Although in the process of diffusion peroxynitrite certainly undergoes reaction with mitochondrial proteins (68), small but sufficient amounts of peroxynitrite may "leak out" from mitochondria (70) to initiate eNOS dysfunction (Fig. 11). Although we did not find eNOS present in the mitochondrial fraction, it is possible that eNOS may be in close proximity to the organelle, thereby creating a compartmentalization of redox signaling that favors the interaction between superoxide and NO as well as peroxynitrite and eNOS. This is supported by the observation that eNOS was reported to be associated to the cytosolic side of the outer mitochondrial membrane (72) or to translocate from the membrane to the mitochondria under certain conditions (73).

Another possibility is that mitochondrial superoxide dismutates to form hydrogen peroxide that freely diffuses in the cytoplasm to activate a superoxide-generating Nox oxidase outside the mitochondria (Fig. 11). This type of regulation is supported by earlier reports showing that Ang II-induced release of hydrogen peroxide by mitochondria functions as an upstream stimulator of cytoplasmic Nox2 in cardiac myocytes and endothelial cells (17–19, 66, 67). Because Nox4 is also present in the membrane in MCs (21), it is tempting to speculate that "membrane" Nox4 may be the enzyme targeted by hydrogen peroxide. The effect of siNox4 on intracellular superoxide generation may be a reflection of its inability to stimulate the superoxide-generating Nox situated downstream following blockade of Nox4-derived hydrogen peroxide production in the mitochondria. This may be particularly relevant in cells like MCs that express multiple Nox homologues (10, 13, 14, 74–77).

Finally, the recent finding that superoxide generated toward the matrix by mitochondrial respiratory chain complex I can be released in the cytosol (78) raises the possibility that Nox4-derived superoxide may exit the mitochondria and react rapidly with NO produced by eNOS in the proximity of the mitochondria (Fig. 11). Further investigations are required to define the mechanisms that integrate Ang II-dependent mitochondrial superoxide generation and the cellular events that occur outside the mitochondria.

In conclusion, we have identified a novel role for Nox4 as an essential mediator of peroxynitrite-dependent eNOS uncoupling and decline in NO bioavailability in response to Ang II. We have also established the significance of this redox pathway in Ang II-mediated MC extracellular matrix accumulation. Our study places Nox4 and mitochondrial ROS as central mediators that control Ang II-induced redox signaling and that lead to eNOS dysfunction and MC fibrotic injury. Specific inhibition of

FIGURE 9. **Overexpression of MnSOD attenuates Ang II-induced decrease in NO bioavailability and fibronectin expression in MCs.** *A*, MCs were infected with AdβGal or AdMnSOD, and expression of MnSOD was assessed in total cell lysate (*Tot*) or Mit fraction by Western blot analysis. Immunoblotting with MnSOD antibody confirmed the overexpression of the enzyme from the adenovirus vector. *B*, after infection with AdMnSOD or AdβGal, mitochondrial ROS production in response to Ang II (1 μM, 10 min or 1 h) was evaluated using MitoSOX Red fluorescence and confocal microscopy. Fluorescence intensity was semiquantified, and the values are the means ± S.E. from three independent experiments. **, $p < 0.01$ *versus* control cell infected with AdβGal. ##, $p < 0.01$ *versus* Ang II in cells infected with AdβGal. *C*, MCs were infected with AdMnSOD or AdβGal and treated with Ang II (10 min or 1 h), and 3-nitrotyrosine staining was assessed with confocal laser microscopy. The values are the means ± S.E. from three independent experiments. **, $p < 0.01$ *versus* control (βGal-infected cells). ##, $p < 0.01$ *versus* Ang II in βGal-infected cells. The photomicrographs are representative of three individual experiments. For each panels, fluorescence intensity was semiquantified. The values are the means ± S.E. from three independent experiments. **, $p < 0.01$ *versus* control (βGal-infected cells). ##, $p < 0.01$ *versus* Ang II in βGal-infected cells. *D*, MCs were infected with AdMnSOD or AdβGal and treated with Ang II (1 or 24 h), and cGMP synthesis was determined. The values are the means ± S.E. from three independent experiments. **, $p < 0.01$ *versus* AdβGal-infected cells. *E* and *F*, after infection with adenovirus encoding AdMnSOD or AdGFP, fibronectin protein expression in response to Ang II (1 μM, 24 h) was evaluated by Western blot analysis (*E*) and immunofluorescence (*F*). In *E*, the immunoblot in the *middle* shows expression of MnSOD from the adenovirus vectors. GAPDH was used as a loading control. *Right panel*, histogram representing the ratio of the intensity of fibronectin bands quantified by densitometry factored by the densitometric measurement of GAPDH band. The data are expressed as percentages of control (cells infected with AdβGal), where the ratio in the control was defined as 100%. The values are the means ± S.E. from three independent experiments. *F*, *right panel*, histogram representing the semiquantification of fluorescence intensity. The photomicrographs are representative of three individual experiments. **, $p < 0.01$ *versus* control cells infected with AdβGal. ##, $p < 0.01$ *versus* Ang II in cells infected with AdβGal.

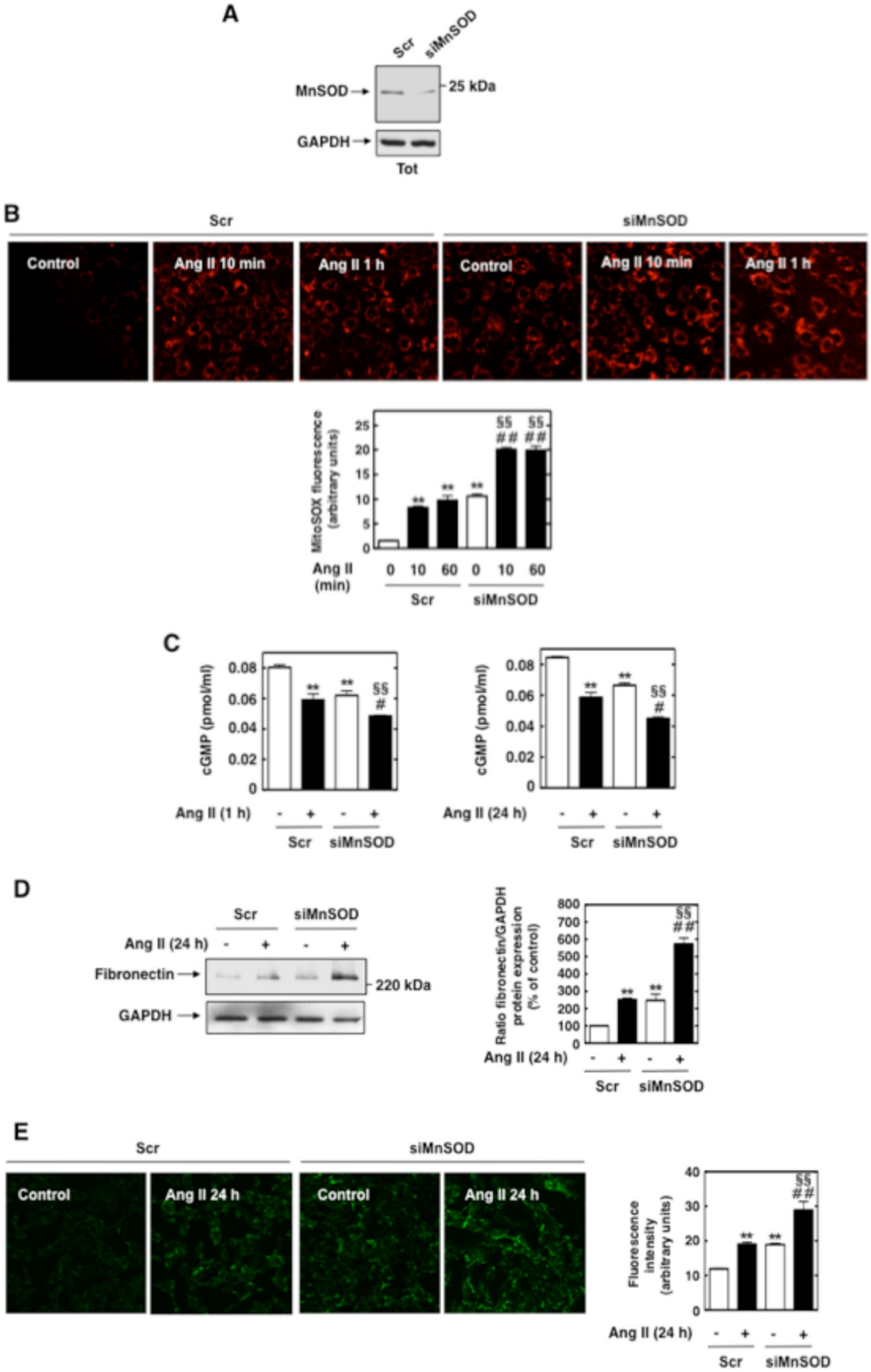

FIGURE 10. **Silencing of MnSOD expression enhances Ang II-induced decrease in NO bioavailability and fibronectin expression in MCs.** *A*, MCs were transfected with Scr or siMnSOD MCs, and expression of MnSOD was assessed in total cell lysate (*Tot*) by Western blot analysis. Immunoblotting with MnSOD antibody confirmed the silencing of the enzyme by siMnSOD. *B*, after transfection with Scr or siMnSOD, mitochondrial ROS production in response to Ang II (1 μM; 10 min or 1 h) was evaluated using MitoSOX Red fluorescence and confocal microscopy. Fluorescence intensity was semiquantified, and the values are the means ± S.E. from three independent experiments. **, $p < 0.01$ *versus* control cell transfected with Scr. ##, $p < 0.01$ *versus* Ang II in cells transfected with Scr. §§, $p < 0.01$ *versus* control cell transfected with siMnSOD. *C*, MCs were transfected with Scr or siMnSOD and treated with Ang II (1 or 24 h), and cGMP synthesis was determined. The values are the means ± S.E. from three independent experiments. **, $p < 0.01$ *versus* Scr-transfected cells. #, $p < 0.05$ *versus* Ang II in cells transfected with Scr. §§, $p < 0.01$ *versus* control cell transfected with siMnSOD. *D* and *E*, after transfection with Scr or siMnSOD, fibronectin protein expression in response to Ang II (1 μM; 24 h) were evaluated by Western blot analysis (*D*) and immunofluorescence (*E*). *D*, *right panel*, histogram representing the ratio of the intensity of fibronectin bands quantified by densitometry factored by the densitometric measurement of GAPDH band. The data are expressed as percentages of control (cells transfected with Scr), where the ratio in the control was defined as 100%. The values are the means ± S.E. from three independent experiments. *E*, *right panel*, histogram representing the semiquantification of fluorescence intensity. The photomicrographs are representative of three individual experiments. **, $p < 0.01$ *versus* control cells transfected with Scr. ##, $p < 0.01$ *versus* Ang II in cells transfected with Scr. §§, $p < 0.01$ *versus* control cell transfected with siMnSOD.

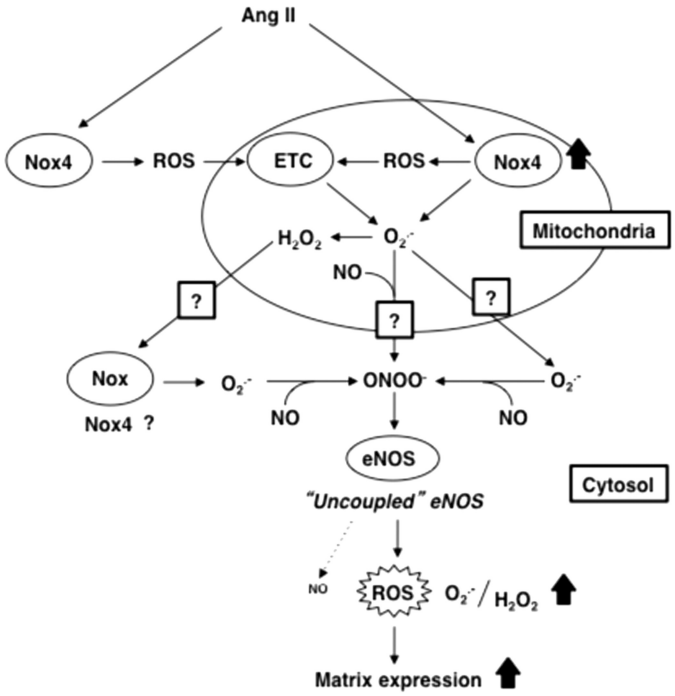

FIGURE 11. **Proposed molecular mechanisms of Ang II-induced fibronectin expression in MCs.** See "Discussion" for details.

this redox pathway, in particular the use of Nox4 inhibitors combined with mitochondria-targeted antioxidants and agents recoupling eNOS, may selectively target several important biological responses to prevent or reverse pathophysiologic manifestations of renal disease, including diabetic nephropathy.

REFERENCES

1. Chatziantoniou, C., and Dussaule, J. C. (2005) Insights into the mechanisms of renal fibrosis. Is it possible to achieve regression? *Am. J. Physiol. Renal Physiol.* **289,** F227–F234
2. Gómez-Guerrero, C., Hernández-Vargas, P., López-Franco, O., Ortiz-Muñoz, G., and Egido, J. (2005) Mesangial cells and glomerular inflammation: from the pathogenesis to novel therapeutic approaches. *Curr. Drug Targets Inflamm. Allergy* **4,** 341–351
3. Fogo, A. B. (1999) Mesangial matrix modulation and glomerulosclerosis. *Exp. Nephrol.* **7,** 147–159
4. Abboud, H. E. (2012) Mesangial cell biology. *Exp. Cell Res.* **318,** 979–985
5. Kim, S., and Iwao, H. (2000) Molecular and cellular mechanisms of angiotensin II-mediated cardiovascular and renal diseases. *Pharmacol. Rev.* **52,** 11–34
6. Kagami S. (2012) Involvement of glomerular renin-angiotensin system (RAS) activation in the development and progression of glomerular injury. *Clin. Exp. Nephrol.* **16,** 214–220
7. Lafayette, R. A., Mayer, G., Park, S. K., and Meyer, T. W. (1992) Angiotensin II receptor blockade limits glomerular injury in rats with reduced renal mass. *J. Clin. Invest.* **90,** 766–771
8. Ruiz-Ortega, M., Rupérez, M., Esteban, V., Rodríguez-Vita, J., Sánchez-López, E., Carvajal, G., and Egido, J. (2006) Angiotensin II. A key factor in the inflammatory and fibrotic response in kidney diseases. *Nephrol. Dial. Transplant.* **21,** 16–20
9. Rincon-Choles, H., Kasinath, B. S., Gorin, Y., and Abboud, H. E. (2002) Angiotensin II and growth factors in the pathogenesis of diabetic nephropathy. *Kidney Int. Suppl.* **82,** S8–S11
10. Nistala, R., Whaley-Connell, A., and Sowers, J. R. (2008) Redox control of renal function and hypertension. *Antioxid. Redox. Signal.* **10,** 2047–2089
11. Barnes, J. L., and Gorin, Y. (2011) Myofibroblast differentiation during fibrosis. Role of NAD(P)H oxidases. *Kidney Int.* **79,** 944–956
12. Lassègue, B., San Martín, A., Griendling, K. K. (2012) Biochemistry, physiology, and pathophysiology of NADPH oxidases in the cardiovascular system. *Circ. Res.* **110,** 1364–1390
13. Gorin, Y., and Block, K. (2013) Nox4 and diabetic nephropathy: With a friend like this, who needs enemies? *Free Radic. Biol. Med.* **61C,** 130–142
14. Gorin, Y., and Block, K. (2013) Nox as a target for diabetic complications. *Clin. Sci.* (*Lond.*) **125,** 361–382
15. Bedard, K., and Krause, K. H. (2007) The NOX family of ROS-generating NADPH oxidases. Physiology and pathophysiology. *Physiol. Rev.* **87,** 245–313
16. Garrido, A. M., and Griendling, K. K. (2009) NADPH oxidases and angiotensin II receptor signaling. *Mol. Cell Endocrinol.* **302,** 148–158
17. Dikalov, S. I., and Nazarewicz, R. R. (2013) Angiotensin II-induced production of mitochondrial reactive oxygen species. Potential mechanisms and relevance for cardiovascular disease. *Antioxid. Redox Signal.* **19,** 1085–1094
18. Dikalov, S. (2011) Cross talk between mitochondria and NADPH oxidases. Dikalov. *Free Radic. Biol. Med.* **51,** 1289–1301
19. Dai, D. F., Rabinovitch, P. S., and Ungvari, Z. (2012) Mitochondria and cardiovascular aging. *Circ. Res.* **110,** 1109–1124
20. Gorin, Y., Block, K., Hernandez, J., Bhandari, B., Wagner, B., Barnes, J. L., and Abboud, H. E. (2005) Nox4 NAD(P)H oxidase mediates hypertrophy and fibronectin expression in the diabetic kidney. *J. Biol. Chem.* **280,** 39616–39626
21. Block, K., Gorin, Y., and Abboud, H. E. (2009) Subcellular localization of Nox4 and regulation in diabetes. *Proc. Natl. Acad. Sci. U.S.A.* **106,** 14385–14390
22. Kim, S. M., Kim, Y. G., Jeong, K. H., Lee, S. H., Lee, T. W., Ihm, C. G., and Moon, J. Y. (2012) Angiotensin II-induced mitochondrial Nox4 is a major endogenous source of oxidative stress in kidney tubular cells. *PLoS One* **7,** e39739
23. Shah, A., Xia, L., Goldberg, H., Lee, K. W., Quaggin, S. E., and Fantus, I. G. (2013) Thioredoxin-interacting protein mediates high glucose-induced reactive oxygen species (ROS) generation by mitochondria and the NADPH oxidase, Nox4, in mesangial cells. *J. Biol. Chem.* **288,** 6835–6848
24. Gorin, Y., Ricono, J. M., Kim, N. H., Bhandari, B., Choudhury, G. G., and Abboud, H. E. (2003) Nox4 mediates angiotensin II-induced activation of Akt/protein kinase B in mesangial cells. *Am. J. Physiol. Renal Physiol.* **285,** F219–F229
25. Block, K., Ricono, J. M., Lee, D. Y., Bhandari, B., Choudhury, G. G., Abboud, H. E., and Gorin, Y. (2006) Arachidonic acid-dependent activation of a p22^{phox}-based NAD(P)H oxidase mediates angiotensin II-induced mesangial cell protein synthesis and fibronectin expression via Akt/PKB. *Antioxid. Redox Signal.* **8,** 1497–1508
26. Block, K., Eid, A., Griendling, K. K., Lee, D. Y., Wittrant, Y., and Gorin, Y. (2008) Nox4 NAD(P)H oxidase mediates Src-dependent tyrosine phosphorylation of PDK-1 in response to angiotensin II. Role in mesangial cell hypertrophy and fibronectin expression. *J. Biol. Chem.* **283,** 24061–24076
27. Alp, N. J., and Channon, K. M. (2004) Regulation of endothelial nitric oxide synthase by tetrahydrobiopterin in vascular disease. *Arterioscler. Thromb. Vasc. Biol.* **24,** 413–420
28. Förstermann, U., and Münzel, T. (2006) Endothelial nitric oxide synthase in vascular disease. From marvel to menace. *Circulation* **113,** 1708–1714
29. Kietadisorn, R., Juni, R. P., and Moens, A. L. (2012) Tackling endothelial dysfunction by modulating NOS uncoupling. New insights into its pathogenesis and therapeutic possibilities. *Am. J. Physiol. Endocrinol. Metab.* **302,** E481–E95
30. Thomas, S. R., Witting, P. K., and Drummond, G. R. (2008) Redox control of endothelial function and dysfunction. Molecular mechanisms and therapeutic opportunities. *Antioxid. Redox Signal.* **10,** 1713–1765
31. Zhao, H. J., Wang, S., Cheng, H., Zhang, M. Z., Takahashi, T., Fogo, A. B., Breyer, M. D., and Harris, R. C. (2006) Endothelial nitric oxide synthase deficiency produces accelerated nephropathy in diabetic mice. *J. Am. Soc. Nephrol.* **17,** 2664–2669
32. Nakagawa, T., Sato, W., Glushakova, O., Heinig, M., Clarke, T., Campbell-Thompson, M., Yuzawa, Y., Atkinson, M. A., Johnson, R. J., and Croker, B. (2007) Diabetic endothelial nitric oxide synthase knockout mice develop advanced diabetic nephropathy. *J. Am. Soc. Nephrol.* **18,** 539–550
33. Kanetsuna, Y., Takahashi, K., Nagata, M., Gannon, M. A., Breyer, M. D., Harris, R. C., and Takahashi, T. (2007) Deficiency of endothelial nitric-

oxide synthase confers susceptibility to diabetic nephropathy in nephropathy-resistant inbred mice. *Am. J. Pathol.* **170,** 1473–1484
34. Satoh, M., Fujimoto, S., Haruna, Y., Arakawa, S., Horike, H., Komai, N., Sasaki, T., Tsujioka, K., Makino, H., and Kashihara, N. (2005) NAD(P)H oxidase and uncoupled nitric oxide synthase are major sources of glomerular superoxide in rats with experimental diabetic nephropathy. *Am. J. Physiol. Renal Physiol.* **288,** F1144–F1152
35. Faria, A. M., Papadimitriou, A., Silva, K. C., Lopes de Faria, J. M., and Lopes de Faria, J. B. (2012) Uncoupling endothelial nitric oxide synthase is ameliorated by green tea in experimental diabetes by re-establishing tetrahydrobiopterin levels. *Diabetes* **61,** 1838–1847
36. Zhang, W., Meng, H., Li, Z. H., Shu, Z., Ma, X., and Zhang, B. X. (2007) Regulation of STIM1, store-operated Ca^{2+} influx, and nitric oxide generation by retinoic acid in rat mesangial cells. *Am. J. Physiol. Renal Physiol.* **292,** F1054–F1064
37. Satoh, M., Fujimoto, S., Arakawa, S., Yada, T., Namikoshi, T., Haruna, Y., Horike, H., Sasaki, T., and Kashihara, N. (2008) Angiotensin II type 1 receptor blocker ameliorates uncoupled endothelial nitric oxide synthase in rats with experimental diabetic nephropathy. *Nephrol. Dial. Transplant.* **23,** 3806–3813
38. Awad, A. S., Webb, R. L., Carey, R. M., and Siragy, H. M. (2004) Renal nitric oxide production is decreased in diabetic rats and improved by AT1 receptor blockade. *J. Hypertens.* **22,** 1571–1577
39. New, D. D., Block, K., Bhandhari, B., Gorin, Y., and Abboud H. E. (2012) IGF-I increases the expression of fibronectin by Nox4-dependent Akt phosphorylation in renal tubular epithelial cells. *Am. J. Physiol. Cell Physiol.* **302,** C122–C130
40. Eid, A. A., Ford, B. M., Block, K., Kasinath, B. S., and Gorin, Y., Ghosh-Choudhury, G., Barnes, J. L., and Abboud, H. E. (2010) AMP-activated protein kinase (AMPK) negatively regulates Nox4-dependent activation of p53 and epithelial cell apoptosis in diabetes. *J. Biol. Chem.* **285,** 37503–37512
41. Zou, M. H., Shi, C., and Cohen, R. A. (2002) Oxidation of the zinc-thiolate complex and uncoupling of endothelial nitric oxide synthase by peroxynitrite. *J. Clin. Invest.* **109,** 817–826
42. Fernandes, D. C., Wosniak, J., Jr., Pescatore, L. A., Bertoline, M. A., Liberman, M., Laurindo, F. R., and Santos, C. X. (2007) Analysis of DHE-derived oxidation products by HPLC in the assessment of superoxide production and NADPH oxidase activity in vascular systems. *Am. J. Physiol. Cell Physiol.* **292,** C413–C422
43. Kashyap, S. R., Roman, L. J., Lamont, J., Masters, B. S., Bajaj, M., Suraamornkul, S., Belfort, R., Berria, R., Kellogg, D. L., Jr., Liu, Y., and DeFronzo, R. A. (2005) Insulin resistance is associated with impaired nitric oxide synthase activity in skeletal muscle of type 2 diabetic subjects. *J. Clin. Endocrinol. Metab.* **90,** 1100–1105
44. Roman, L. J., Sheta, E. A., Martasek, P., Gross, S. S., Liu, Q., and Masters, B. S. (1995) High-level expression of functional rat neuronal nitric oxide synthase in *Escherichia coli*. *Proc. Natl. Acad. Sci. U.S.A.* **92,** 8428–8432
45. Feliers, D., Chen, X., Akis, N., Choudhury, G. G., Madaio, M., and Kasinath, B. S. (2005) VEGF regulation of endothelial nitric oxide synthase in glomerular endothelial cells. *Kidney Int.* **68,** 1648–1659
46. Xia, Y. (2007) Superoxide generation from nitric oxide synthases. *Antioxid. Redox Signal.* **9,** 1773–1778
47. Mount, P. F., and Power, D. A. (2006) Nitric oxide in the kidney. Functions and regulation of synthesis. *Acta Physiol.* (*Oxf.*) **187,** 433–446
48. Wang, S., Shiva, S., Poczatek, M. H., Darley-Usmar, V., and Murphy-Ullrich, J. E. (2002) Nitric oxide and cGMP-dependent protein kinase regulation of glucose-mediated thrombospondin 1-dependent transforming growth factor-β activation in mesangial cells. *J. Biol. Chem.* **277,** 9880–9888
49. Landmesser, U., Dikalov, S., Price, S. R., McCann, L., Fukai, T., Holland, S. M., Mitch, W. E., and Harrison, D. G. (2003) Oxidation of tetrahydrobiopterin leads to uncoupling of endothelial cell nitric oxide synthase in hypertension. *J. Clin. Invest.* **111,** 1201–1209
50. Martyn, K. D., Frederick, L. M., von Loehneysen, K., Dinauer, M. C., and Knaus, U. G. (2006) Functional analysis of Nox4 reveals unique characteristics compared to other NADPH oxidases. *Cell Signal.* **18,** 69–82
51. Takac, I., Schröder, K., Zhang, L., Lardy, B., Anilkumar, N., Lambeth, J. D., Shah, A. M., Morel, F., and Brandes, R. P. (2011) The E-loop is involved in hydrogen peroxide formation by the NADPH oxidase Nox4. *J. Biol. Chem.* **286,** 13304–13313
52. Dikalov, S. I., Dikalova, A. E., Bikineyeva, A. T., Schmidt, H. H., Harrison, D. G., and Griendling, K. K. (2008) Distinct roles of Nox1 and Nox4 in basal and angiotensin II-stimulated superoxide and hydrogen peroxide production. *Free Radic. Biol. Med.* **45,** 1340–1351
53. Brandes, R. P., Takac, I., and Schröder, K. (2011) No superoxide–no stress? Nox4, the good NADPH oxidase! *Arterioscler. Thromb. Vasc. Biol.* **31,** 1255–1257
54. Zhang, M., Perino, A., Ghigo, A., Hirsch, E., and Shah, A. M. (2013) NADPH oxidases in heart failure. Poachers or gamekeepers? *Antioxid. Redox Signal.* **18,** 1024–1041
55. Schröder, K., Zhang, M., Benkhoff, S., Mieth, A., Pliquett, R., Kosowski, J., Kruse, C., Luedike, P., Michaelis, U. R., Weissmann, N., Dimmeler, S., Shah, A. M., and Brandes, R. P. (2012) Nox4 is a protective reactive oxygen species generating vascular NADPH oxidase. *Circ. Res.* **110,** 1217–1225
56. Craige, S. M., Chen, K., Pei, Y., Li, C., Huang, X., Chen, C., Shibata, R., Sato, K., Walsh, K., and Keaney, J. F., Jr. (2011) NADPH oxidase 4 promotes endothelial angiogenesis through endothelial nitric oxide synthase activation. *Circulation* **124,** 731–740
57. Dikalova, A. E., Góngora, M. C., Harrison, D. G., Lambeth, J. D., Dikalov, S., and Griendling, K. K. (2010) Upregulation of Nox1 in vascular smooth muscle leads to impaired endothelium-dependent relaxation via eNOS uncoupling. *Am. J. Physiol. Heart Circ. Physiol.* **299,** H673–H679
58. Youn, J. Y., Gao, L., and Cai, H. (2012) The $p47^{phox}$- and NADPH oxidase organiser 1 (NOXO1)-dependent activation of NADPH oxidase 1 (NOX1) mediates endothelial nitric oxide synthase (eNOS) uncoupling and endothelial dysfunction in a streptozotocin-induced murine model of diabetes. *Diabetologia* **55,** 2069–2079
59. Zhang, M., Song, P., Xu, J., and Zou, M. H. (2011) Activation of NAD(P)H oxidases by thromboxane A2 receptor uncouples endothelial nitric oxide synthase. *Arterioscler. Thromb. Vasc. Biol.* **31,** 125–132
60. Xu, J., Xie, Z., Reece, R., Pimental, D., and Zou, M. H. (2006) Uncoupling of endothelial nitric oxidase synthase by hypochlorous acid. Role of NAD(P)H oxidase-derived superoxide and peroxynitrite. *Arterioscler. Thromb. Vasc. Biol.* **26,** 2688–2695
61. Cucoranu, I., Clempus, R., Dikalova, A., Phelan, P. J., Ariyan, S., Dikalov, S., and Sorescu, D. (2005) NAD(P)H oxidase 4 mediates transforming growth factor-β1-induced differentiation of cardiac fibroblasts into myofibroblasts. *Circ. Res.* **97,** 900–907
62. Lyle, A. N., Deshpande, N. N., Taniyama, Y., Seidel-Rogol, B., Pounkova, L., Du, P., Papaharalambus, C., Lassègue, B., and Griendling, K. K. (2009) Poldip2, a novel regulator of Nox4 and cytoskeletal integrity in vascular smooth muscle cells. *Circ. Res.* **105,** 249–259
63. Spencer, N. Y., Yan, Z., Boudreau, R. L., Zhang, Y., Luo, M., Li, Q., Tian, X., Shah, A. M., Davisson, R. L., Davidson, B., Banfi, B., and Engelhardt J. F. (2011) Control of hepatic nuclear superoxide production by glucose 6-phosphate dehydrogenase and NADPH oxidase-4. *J. Biol. Chem.* **286,** 8977–8987
64. Giacco, F., Brownlee, M. (2010) Oxidative stress and diabetic complications. *Circ. Res.* **107,** 1058–1070
65. Dikalova, A. E., Bikineyeva, A. T., Budzyn, K., Nazarewicz, R. R., McCann, L., Lewis, W., Harrison, D. G., and Dikalov, S. I. (2010) Therapeutic targeting of mitochondrial superoxide in hypertension. *Circ. Res.* **107,** 106–116
66. Doughan, A. K., Harrison, D. G., and Dikalov, S. I. (2008) Molecular mechanisms of angiotensin II-mediated mitochondrial dysfunction. Linking mitochondrial oxidative damage and vascular endothelial dysfunction. *Circ. Res.* **102,** 488–496
67. Dai, D. F., Johnson, S. C., Villarin, J. J., Chin, M. T., Nieves-Cintrón, M., Chen, T., Marcinek, D. J., Dorn, G. W., 2nd, Kang, Y. J., Prolla, T. A., Santana, L. F., and Rabinovitch, P. S. (2011) Mitochondrial oxidative stress mediates angiotensin II-induced cardiac hypertrophy and Galphaq overexpression-induced heart failure. *Circ. Res.* **108,** 837–846
68. Radi, R., Cassina, A., Hodara, R., Quijano, C., and Castro, L. (2002) Peroxynitrite reactions and formation in mitochondria. *Free Radic. Biol. Med.* **33,** 1451–1464

69. Gus'kova, R. A., Ivanov, I. I., Kol'tover, V. K., Akhobadze, V. V., and Rubin, A. B. (1984) Permeability of bilayer lipid membranes for superoxide (O_2^-) radicals. *Biochim. Biophys. Acta* **778,** 579–585
70. Martínez-Ruiz, A., Cadenas, S., and Lamas, S. (2011) Nitric oxide signaling. Classical, less classical, and nonclassical mechanisms. *Free Radic. Biol. Med.* **51,** 17–29
71. Denicola, A., Souza, J. M., Radi, R., and Lissi E. (1996) Nitric oxide diffusion in membranes determined by fluorescence quenching. *Arch. Biochem. Biophys.* **328,** 208–212
72. Gao, S., Chen, J., Brodsky, S. V., Huang, H., Adler, S., Lee, J. H., Dhadwal, N., Cohen-Gould, L., Gross, S. S., and Goligorsky, M. S. (2004) Docking of endothelial nitric oxide synthase (eNOS) to the mitochondrial outer membrane. A pentabasic amino acid sequence in the autoinhibitory domain of eNOS targets a proteinase K-cleavable peptide on the cytoplasmic face of mitochondria. *J. Biol. Chem.* **279,** 15968–15974
73. Rafikov, R., Rafikova, O., Aggarwal, S., Gross, C., Sun, X., Desai, J., Fulton, D., and Black, S. M. (2013) Asymmetric dimethylarginine induces endothelial nitric oxide synthase mitochondrial redistribution through the nitration-mediated activation of Akt1. *J. Biol. Chem.* **288,** 6212–6226
74. Plesková, M., Beck, K. F., Behrens, M. H., Huwiler, A., Fichtlscherer, B., Wingerter, O., Brandes, R. P., Mülsch, A., and Pfeilschifter, J. (2006) Nitric oxide down-regulates the expression of the catalytic NADPH oxidase subunit Nox1 in rat renal mesangial cells. *FASEB J.* **20,** 139–141
75. Li, Y., and Wang, S. (2010) Glycated albumin activates NADPH oxidase in rat mesangial cells through up-regulation of $p47^{phox}$. *Biochem. Biophys. Res. Commun.* **397,** 5–11
76. Miyata, K., Rahman, M., Shokoji, T., Nagai, Y., Zhang, G. X., Sun, G. P., Kimura, S., Yukimura, T., Kiyomoto, H., Kohno, M., Abe, Y., and Nishiyama, A. (2005) Aldosterone stimulates reactive oxygen species production through activation of NADPH oxidase in rat mesangial cells. *J. Am. Soc. Nephrol.* **16,** 2906–2912
77. Radeke, H. H., Cross, A. R., Hancock, J. T., Jones, O. T., Nakamura, M., Kaever, V., and Resch, K. (1991) Functional expression of NADPH oxidase components (α- and β-subunits of cytochrome b_{558} and 45-kDa flavoprotein) by intrinsic human glomerular mesangial cells. *J. Biol. Chem.* **266,** 21025–21029
78. Lustgarten, M. S., Bhattacharya, A., Muller, F. L., Jang, Y. C., Shimizu, T., Shirasawa, T., Richardson, A., and Van Remmen, H. (2012) Complex I generated, mitochondrial matrix-directed superoxide is released from the mitochondria through voltage dependent anion channels. *Biochem. Biophys. Res. Commun.* **422,** 515–521